JANUARY 2018

M.Sc. in Physics Engineering

HASAN RAAD AHMED

**UNIVERSITY OF GAZIANTEP**

**GRADUATE SCHOOL OF**

**NATURAL AND APPLIED SCENCES**

# INVESTIGATION OF THERMOLUMINESCENCE PROPERTIES OF NATURAL CALCITE ($CaCO_3$) FROM IRAQ

**M.Sc. THESIS**

**IN**

**ENGINEERING PHYSICS**

**BY**

**HASAN RAAD AHMED**

**JANUARY 2018**

# Investigation of Thermoluminescence Properties of Natural Calcite ($CaCO_3$) from Iraq

**M.Sc. Thesis**

**in**

**Physics Engineering**

**University of Gaziantep**

**Supervisor**

**Assoc. Prof. Dr. Rabia Güler YILDIRIM**

**By**

**Hasan Raad AHMED**

**January 2018**

REPUBLIC OF TURKEY
UNIVERSITY OF GAZİANTEP
GRADUATE SCHOOL OF NATURAL & APPLIED SCIENCES
DEPARTMENT OF ENGINEERING PHYSICS

Name of the thesis: Investigation of Thermoluminescence Properties of Natural Calcite ($CaCO_3$) from Iraq

Name of the student: Hasan Raad AHMED

Exam date: 31.01.2018

Approval of the Graduate School of Natural and Applied Sciences

Prof. Dr. Ahmet. Necmeddin YAZICI

Director

I certify that this thesis satisfies all the requirements as a thesis for the degree of Master of Science.

Prof. Dr. Ramazan KOC

Head of Department

This is to certify that we have read this thesis and that in our opinion it is fully adequate, in scope and quality, as a thesis for the degree of Master of Science.

Assoc. Prof Dr. Rabia Güler YILDIRIM

Supervisor

| Examining Committee Members | Signature |
|---|---|
| Assoc. Prof. Dr. R. Güler YILDIRIM | ---------- |
| Assoc. Prof. Dr. Vural E. KAFADAR | ---------- |
| Assoc. Prof. Dr. Tuba DENKCEKEN | ---------- |

**Hereby declare that all information in this document has been obtained and presented in accordance with academic rules and ethical conduct. I also declare that, as required by these rules and conduct, I have fully cited and referenced all material and results that are not original to this work**.

**Hasan Raad AHMED**

## ABSTRACT

### INVESTIGATION OF THERMOLUMINESCENCE PROPERTIES OF NATURAL CALCITE ($CaCO_3$) FROM IRAQ

**AHMED, Hasan Raad**

**M.Sc. in Engineering Physics**

**Supervisor: Assoc. Prof Dr. R. Güler YILDIRIM**

**January 2018**

**59 Pages**

Thermoluminescnce characteristics for natural calcite sample has been investigated in this study after irradiated by beta source for dose level from 2.4 Gy to 2.3 kGy. Computer glow curves deconvolution (CGCD) and Peak shape (PS) methods are used to estimate E (activation energy), s (attempt-to-escape frequency factor) and b (kinetic order).

Calcite sample which used in this study where collected from DOHUK city – north of Iraq show two peaks follow Beta irradiation for dose levels which were applied in this study, peak 1 at 189 $^0$C and peak 2 at 280 $^0$C.

Benefits of studying dose response and fading are to measure irradiation dosimetry and archeological dating. Calcite sample was irradiated and stored in dark box at room temperature and read out, after three weeks peak 1 completely disappeared, after 1 hour of stored peak 1 down to half of original intensity value, this means that this sample loses radiation fairly quickly.



**Keywords:** Thermoluminescnce; Annealing; Unannealing; Kinetics parameters; Calcite.

## ÖZET

## IRAK KALSIT'IN (CACO3) TERMOLOMINANS ÖZELLIKLERININ ARAŞTIRILMASI

**AHMED, Hasan Raad**

**Yüksek Lisans Tezi, Fizik Mühendisliği Bölümü**

**Tez Yöneticisi: Doç.Dr. R. Güler YILDIRIM**

**Ocak 2018**

**59 Sayfa**

Bu çalışmada doğal kalsit numinesinin termoluminesans karakteristiği 24 Gy den 2.3 kGy lik beta dozlaması ile çalışılmıştır. Aktivasyon enerjisi (E), frekans faktörü (s) ve kinetik derecesi (b), ışıldama eğrisi ayrışımı (CGCD), eğri şekili (PS) ve methoudu ile belirlenmiştir

Kuzay Irak, Duhok şehrinden alınan kalsit örneği beta dozloması ile 189 ºC ve 280 ºC de iki ışıldama eğrisi tepeciği göstermiştir.

Radyasyon dozimetresinde ve arkeolojik yapı tayinlerinde oldukça kullanışlı olan doz tepkisi eğrisi ve zaman ile sönüm methodu kullanılan materyal için incelenmiştir.

Kalsit numinesinin dozlandıktan sonra karanlık bir ortamdan üç hafta bekletildikten sonra birinci ışıldama tepeciği tamamen kaybolmuştur. Birinci ışıldama tepeciği bir saat bekledikten sonra orijinal değerinin yarısına azalmıştır, bu demektir ki kalsit numinesi radyasyonu hızlı bir şekilde kaybediyor.



**Anhtar kelimeler:** Termoluminesans, Tavlama, Kinetik parametreleri, Kalsit.

TO MY FAMILY

FATHER, MOTHER, BROTHERS AND SISTERS

TO MY FRIENDS

I OFFER MY SUCCESS

HASAN

## ACKNOWLEDGEMENT

My heartfelt thanks and deep gratitude to my supervisor Assoc. Prof Dr. R. Güler YILDIRIM for the continuous support of my M.Sc, study and research, for ongoing advice, encouragements.

My gratitude to the head and staff engineering of the Physics Department in the College of Science for their assistant and support during my study and research.

Also, my heartfelt Thanks for my Family and Friends who encouraged and supported me to complete my study.

## TABLE OF CONTENTS

**Page**

## LIST OF FIGURES

**Page**

## LIST OF TABELS

**Pages**

## LIST OF SYMBOLS

$A_h$: recombination transition coefficient for electrons in the conduction band

$A_n$: transition coefficient for electrons in the conduction band

$A_m$: transition coefficient for electrons in the conduction band to the deep traps

b: order of kinetic

β: heating rate

E: Energy

$E_a$: activation energy

I: thermoluminescence intensity

k: Boltzman's Constant

n: concentration of electrons in the electron traps concentration of electrons in the conduction band

$n_c$: concentration of holes in the recombination centers

$n_h$: concentration of holes in the valance band

$n_o$: initial concentration of trapped electrons

N: concentration of available electron traps

$N_h$: concentration of available hole centers

m: concentration of electrons in the deep traps

M: concentration of available deep traps

p: probability per unit time of the release of an electron from the trap

s: frequency factor or pre-exponential factor

T: temperature

$T_m$: peak temperature

# CHAPTER 1

# INTRODUCTION

## 1.1 Luminescence phenomena

Luminescence is the emission of light from a part of a solid called phosphor, and this emitted light, with the exception of black body radiation, is converted to solid energy by some previous excitation of the solid electronic system to separate. This storage capacity is essential in luminescence dosimetry and is usually associated with the presence of an activator.

In the below table shows the luminescence and excitation methods [1].

**Table 1.1** Compare between luminescence and excitation methods

| LUMINESCENCE PHENOMENA | METHOD OF EXCITATION |
|---|---|
| Bioluminescence | Biochemical reactions |
| Cathodoluminescence | Electron beam |
| Chemiluminescence | Chemical reactions |
| Electroluminescence | Electric field |
| Photoluminescence | U. V. and infrared light |
| Piezoluminescence | Pressure (10 tons $m^2$) |
| Triboluminescence | Friction |
| Radioluminescence | Ionising radiation |
| Sonoluminescence | Sound waves |
| Fluorescence<br>Phosphorescence<br>Thermoluminescence<br>Lyoluminescence | Ionizing radiation, U.V. and visible light |

In particular, when the material absorbs some of the radiation, According to Stoke's law, the light will be emit with long wavelength. Moreover, the wavelength of the transmitted light is a symbol of the material.

Luminescence knew as energy expended by the element as light, after the absorption of energy from the suppressing source, which stimulates the rise of the electron from its basic energy level to another, identical to the greater energy. When light is emitted, if the electron falls to the ground energy level it can be classified according to the characteristic time t between excitation energy absorption and emission [2].

The luminescence center is an atom or group of atoms called an activator located within the lattice of the host material and acts as a separate center for local absorption of the excitation energy. Otherwise, the luminescent center is the quantum state in the band gap of the insulator, which serves as the center of recombination of the charge carriers, if the carrier is captured and another carrier of the opposite sign is also held for a certain time until it is also trapped for a certain period of time , Both are combined. This recombination causes excessive energy emission as a photon or phonon [3].

**1.2 Thermoluimnescence (TL)**

From an infinitesimal point of view, Thermoluminescence entails of perturbations in the electronic organization of insulating or semiconducting materials, from thermodynamic equality by absorption of internal energy. Then the system's thermal relaxation, back to a steady state. In principle, thermolumnescence is the photoexcitation of a temperature-excited crystal from the mineral after subtraction of the excitation (ionizing radiation); Thermoluminescence is the case of phosphorescence observed under conditions of stable heat rise [4].

Thermoluminescence properties of crystal commonly were studied. Calcite is one of the most common and widespread minerals found in the limestone deposit which is very common sedimentary rock. The structure of calcite is hexagonal. Calcite structures have been defined as NaCl-type arrangements of (Ca) cations and ($CO_3$) anions. Examples of nonconductor are cubic structure alkali halides, such LiF and NaCl. The Thermoluminescence (TL) calcite ($CaCO_3$) crystal of trigonal symmetry)

has been studied by several workers. Thermoluminescence (TL) has become an important method for the dating of archaeological and geological materials. Furthermore, an important material in Thermoluminescence dosimetry (TLD), which is mainly an insulator, is due to radiation energy in which electrons are completely absorbed. Many of calcite studies indicate that TL properties also depend on the type of impurity. Also the type of impurities and its density will affect to thermoluminscence sensitivity and glow shape on artificially grown (CaCO3) crystals. Therefore, the definition of kinetics parameters is an active field of research and has developed various methods for controlling the parameters of the luminescence curve [5].

### 1.3 Definition of some terms

#### 1.3.1 Activation energy

The energy "E" is expressed in eV, and is forbidden to assign the band gap to the metastable state or energy level between the conduction band of the crystal and the valence band. This energy is also the depth of the isotopathy trap. The metastable energy levels are electron traps near CB, hole traps above VB, central emission centers of forbidden bands [6].

Metastable levels are the result of disorganization of the crystal construction. Crystals can contain various traps and luminescent centers. If E > several kT, (k is the Boltzmann's constant), that is mean the trapped charge will stay at the traps for a long time [7].

Hitting the sample with ionizing radiation produces a free charge that can be trapped in metastability. Suppose the previously excited sample is heated to provide a certain amount of energy in the form of thermal energy and the trapped charge can be released from the trap.

It is easy to see that "$T_{m.}$" will increases when "E" increases. In fact, in the case of $E >> kT_m$, $T_M$ increases almost linearly with ".E.". This behavior is consistent with the "Randall-Wilkins" model which requires deeper energy and higher temperature to capture electrons for deeper traps [8, 9].

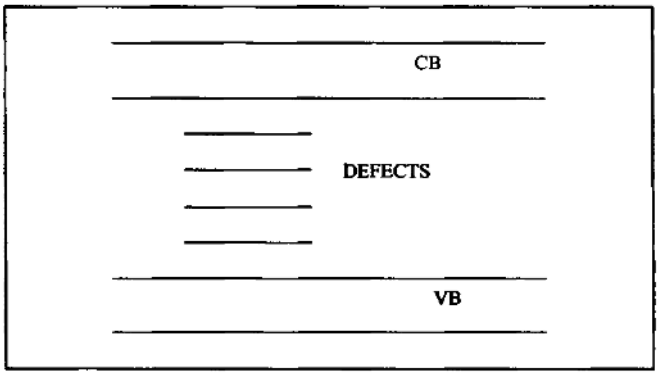


**Figure 1.1** Simple energy band structure with defect band gap.

### 1.3.2 Annealing

Annealing is the heat treatments that needs to be made from a diameter material. Some thermo luminescent materials require complicated annealing procedures and "LiF: Mg, Ti" is one of that material. It needs high temperature annealing, then low temperature annealing.

In general, high temperature annealing is to remove dose traps of residual signals that can cause poor background during the next use of the dosimeter. Cryogenic annealing requires stabilization and aggregation of cryogenic traps to increase the sensitivity of the main dosimetry trap and reduce the signal loss inasmuch to radiation due to thermal or optical fading during use [10]. The TL characteristic exhibited by the phosphor is strongly dependent on the type of thermal anneal experienced before irradiation. In general, more defects occur at higher annealing temperatures. Cooling rate also affect in the number of defects when it used to cool phosphor to ambient temperature [11].

### 1.3.3 Frequency factor, *s*

The frequency factor "s", known as the electrons attempts to escapes from the traps, is interpreted as the numbers of times to escapes per seconds "v", the lattice reaction of electrons with the solid, multiplied by the transitions probability K, multiplied by this terms to explain the entropy changes ΔS from trap transition to delocalized band the change. s can be expressed as :

$$\boldsymbol{s = v.k\,exp\left(\frac{\Delta S}{k}\right)}$$

Where "k" is the Boltzmann constants.

s value must be same to the frequency of lattice vibrational (Debye frequency), i.e. $10^{12}$-$10^{14}$ $s^{-1}$ the possible range of s according to Chen is from $10^5$ to $10^{13}$ $s^{-1}$ [12-13].

The meanings of the frequency factors given by "Randall and Wilkins" are as follows: They describe the traps as a potential wells and "s" must be the product of the frequency of the well electron breakdown barrier and the reflection coefficient. As previously stated, one should be able to predict the magnitude of the crystal vibration frequency, i.e. $10^{12}$ $s^{-1}$.

Alternatively, s should be considered to be related to the sections "σ" of the trap by the following relation:

$$\boldsymbol{s = v_e . N_e \delta}$$

Where $v_e$ is the thermal velocity of the electrons at CB, $N_c$ Whether the electronic level is available near the undermost of the conduction bands, and "$\boldsymbol{\delta}$" is the captured cross sections of the traps. In this case, the values of "s" vary from $10^8$ to $10^{14}s^{-1}$. In some cases, the frequency factors as well as the exponentials factor can be considered temperature-dependents and proportional to "α", with a between -2 and +2.

### 1.3.4 Glow curve

It is the graph of the Thermoluminescence intensity, I, as a function of the temperature when it read out. Each trapping level in the sample gives growth to associated glow peak; so, a glow curve can be formed by many peaks, each concerning to dissimilar trapping levels. These peaks can be determined or not determined on the luminescence curve.

### 1.3.5 Interactive traps

Electrons emanating from surface traps can be captured by deep traps (thermal traps): this trap is called interactive. Deep Trap Opposite Trap shallow traps release electrons from the recombination center.

### 1.3.6 Kinetics order: effects on the glow-curve shape

The effective influence of the order of the kinetics on the shape of the radiance is expressed in Fig. 1.2, in which two glow curves are compared from one type of trap.

In the case of second-order kinetic, $T_M$ rises on the order of 1% and senses the temperature at the primary peak maximum. The main difference is that light is emitted at a higher temperature than $T_m$, as the trap retards the emission of electrons. Also, with the fixed value of E, $T_m$ increases as β decreases and decreases with a fixed value β, the result of $T_m$ is proportional to E [9].

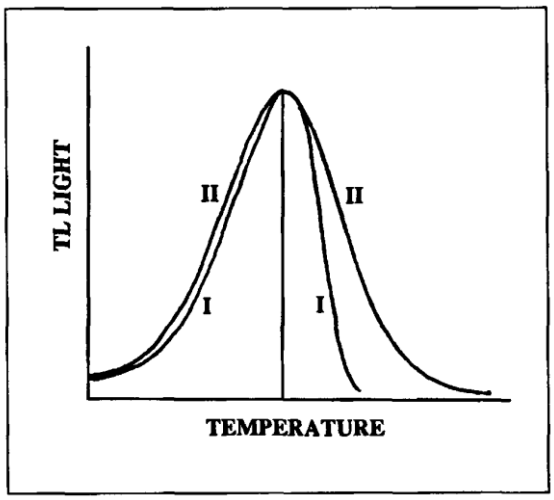


**Figure 1.2** Glow-peak shapes for 1st order (I) and 2nd order (II) [9]

# CHAPTER 2

# LITERATURE SURVEY

Ki-Bum et al. [14] used Korean calcite to study characteristics of overlapping peaks. These properties can provide useful insights into the determination of radiation dosimeters and luminescence dating. In the $T_m$-$T_{stop}$ method, the numbers of concealed glow peaks, the kinetic parameters of the separated glow peaks, thermal activation energy, kinetic orders, and frequency factor were measured using the CGCD method. This method shows the luminescence curve of the calcite composition of at least four peaks (P1 to P4) in the temperature range (room temperature to 450 °C), and when a bleaching experiment using the solar simulator and P4 is used for thermally stable peaks P3, the exponential the decay of the tug was accompanied by rapid initial bleaching, the peak of P4 bleached exponentially, but slowly reached the residual level. As a result of bleaching, the intensity of peaks P3 and P4 decreased to about 4% and 30% of the original value, respectively. On the other hand, the TL signal for P3 and p4 show a linear increases up to maximums doses investigated, 520 Gy, with nuance in shape of growths curves. The life time of peak P3 was calculated as $5.20*10^5$ year, when it was $6.39*10^{11}$ year for peak P4 The shapes of growths curves and life time estimated for the alienated peaks p3 and p4 point out their interest for TL dating.

Yassin A.Abdel-Razak [15] used natural calcite to investigate Thermoluminescence dosimeter. The sample of calcite collected from El-Bakriya Eastern Desert, Egypt. This study was to investigate feasibility for use in gamma radiation dosimeter. At temperature of 283 $^oC$ a peak appeared on the glow curve was found to have a linear response to doses over the range 0.05 – 1000 Gy, predominantly after being annealed at 600 $^oC$ for 5 hours before irradiation. The activation energy for the traps which produced peak at 283 $^oC$ has no effect by annealing and irradiation, for this reason, this sample of calcite specified as a good dosimeters for many diametric applications.

R. Guler Yildirim et al. [16]. Studied thermolumnescent glow peaks of natural

calcites. The calcite sample which used in this study after beta irradiation at temperature between RT and 350 ºC is superposition of at least four glow peaks, and the glow curve of this calcite sample have two main peaks. The samples were irradiated at diverse dose from 24 Gy to 2.3 KGy to test dose-dependence effect on the peak positions. Trapping parameters estimated from TMP, the results were at maximum intensity for P1 at 115 ºC and 254 ºC for P4 up to 10% of the maximum intensity.

Birol Engin et al. [17]. The feasibility of gamma ray dosimetry using naturally occurring calcites was studied. Annealing above 350 °C increased the sensitivity of all radiation-induced TL peaks, except for glow peaks above 300 °C. On the other hand, the TL sensitivity decreases when annealed in air at 700 °C. The increase in efficiency of TL was found to be dependent on temperature and annealing time. Heating at 600 °C for 5 hours and quenching in ambient air is the optimal condition for increasing TL sensitivity in the studied calcite material. These results are explained using the energy scheme of Zimmerman's pre-dose model (1971) and the rearrangement of impurities in the lattice caused by heating. The values of kinetic parameters E, s and b of the TL glow peak of the annealed sample were found to remain unchanged. TL dose-response curves of stable dose peaks of annealed and unannealed calcite samples are the same linear mathematical function. This means that the annealing process may not change the nature of the capture center except at cryogenic temperature peaks at 125 and 160 °C. The TL dosimetric parameters after calcite annealing were also studied in detail, including glow curves, fading characteristics, dose response, dose rate response, and energy response. The annealed calcite samples were found to respond linearly to gamma rays between 0.05 and 104 Gy.

M.Urbina et al. [18] examined the effect of the calcite dose. The study of Thermoluminescence at different dose rates of gamma and beta radiation in this study has been performed in previous calcite samples - irradiated at a constant dose rate for a long time after irradiation, and the resulting relative population at the center seems Is the last time the characteristics of exposure. The opposite effect is also observed. In fact, the study described the homeostasis of dose-rate effects during irradiation between F and M centers. A second important consequence of the dose-dependent rat effect may be to calculate the previous gamma dose applied to the calcite sample if these doses were to be optically bleached by daylight exposure.

J.M. Kalita et al. [21] thermoluminescence (TL) of natural light pale orange calcite ($CaCO_3$) mineral in fine powder form was studies by room temperature X-ray and UV irradiation of various irradiation times. TL was recorded at a linear ramp rate (2 K / s) from room temperature (300 K) to 523 K. Activated energy, kinetic order, frequency factor and other capture parameters were evaluated by a (CGCD) technique. The three electrons traps centers are estimated to have a conduction band depth of 0.70, 1.30 and 1.49 eV. Studies of the emission spectra recorded at different temperature s showed that there was a single recombination center at a depth of 2.74 eV from the CB. Clear peaks with lower activation energy (0.60 eV) were observed for X-irradiated samples at relatively high temperature (360 K) due to electron-assisted tunneling and subsequent center-to-centers recombination. Under UV excitation there is a sign of phototransmission phenomena where a low TL intensity may be observed; however, it was found that TL intensity increases with UV irradiation time by simultaneous excitation of electrons from the valences bands to the traps level.

Z.S. Macedo, et al. [22] in this work, the "Thermoluminescence properties of doped calcite crystals were studied". The sample is doped with $Mn^{2+}$, $Mg^{2+}$ or $Sr^{2+}$ and more or less than one of these impurities are doped individually or simultaneously. In order to study the effect of impurities on the TL glow peak of calcite, TL glow curve, partial heating measurement, isometry, emission spectra and heat treatment were performed. The conclusion was that the crystals doped with $Mn^{2+}$ showed five TL peaks whose emission spectrum was due only to $Mn^{2+}$. The relative intensities of these peaks are closely related to other divalent dopants ($Sr^{2+}$ or $Mg^{2+}$) added to the solution. These results indicate that although $Sr^{2+}$ and $Mg^{2+}$ act as TL activators to stabilize slightly different electron traps, they are not directly linked to the $Mn^{2+}$ luminescent center.

# CHAPTER 3

# THEORY OF THERMO LUMINESCENCE

## 3.1 Luminescence Phenomena

Luminescence is the discharge of light by a substance that has not been heated, as in fluorescence and phosphors. This discharge releases the energy stored in the solid by a previous specific type of stimulation of the solid electronic system and this discharge does not include blackbody radiation. This reserve capability is very important in the dosimetry of luminescence and basically correlates with the existence of activators [23]. Unlike natural radioactivity, luminescence doesn't take place impulsively; instead, it normally needs energy to stimulate it. The stimulation can be induced by x-rays, gamma rays, ultra violet lights, electrons or alpha particles, all of which can place energy into material that is therefore re-emitted in the form of apparent light. Luminescence's features can be acquired from different kinds of materials [3].

The discharged light can be distinguished according to a specific time, when the electron comes back to its ground energy level between the absorption of the stimulated energy and the discharge of the light. The luminescence will be called fluorescence if this time is less than $10^{-8}$ seconds. In this case, the light is discharged with a wavelength bigger than the wavelength of the absorbed light owing to the scattering of the energy by the molecule. Whereas if the time between the absorption and the discharge is bigger than $10^{-4}$ seconds, the luminescence then is called phosphorescence. The phosphorescence process is clarified with the existence of a metastable level, between the essential and the stimulated levels, which acts as a trap for the electron [3, 9].

## 3.2 Crystal Structures and Crystal Defects

### 3.2.1 Alkali Halides and $CaCO_3$ (Calcite)

The alkalis are distinctive ionic compounds and their physical properties are generally well-known. The greater part of the alkali halides take shape in the rock salt

form, as shown in Figure 3.1. Each cation (alkali metal ion $M^+$) in this form is surrounded by six very close anions (halogen ions $X^-$) and each by six near-neighbor cations. The cations and the anions are each located on the points of unconnected face-centered cubic grids, and those two grids are mutually interleaved.

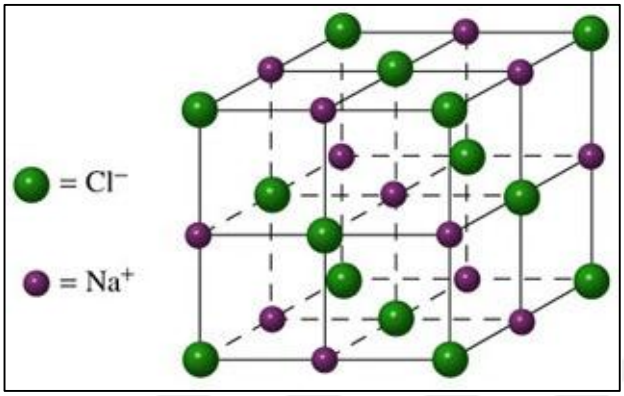


**Figure 3.1** The structure of the rock salt (NaCl) type alkali halide.

When you mix the slightest amount of any chemical defilement with the alkali halides, even in parts-per-million (ppm) the physical and chemical properties of the alkali halides will be affected.

Moreover, raising the temperature will result in a rapid increase in the electric conductivity. The bearers of the electric charges are naturally ionic, not electronic. An insulator, similar to an alkali halide, can be portrayed mechanically by the band model. For a crystal without grid defect, there are no vitality levels between the valance and conduction bands. The energy levels presented might be detached, or might be disseminated relying upon the correct way of the defect and of the host grid. By and large terms, it is trusted that the grid flaws, defilement, inherent and outward imperfections offer ascent to localized energy levels (meta stable state) inside the forbidden energy gap and they might be surely known utilizing the case of an alkali halide crystal of the kind $M^+X^-$. Calcite is a standout amongst the most well-known and broad minerals found in limestone deposits which is depicted as a NaCl type arranged as ($Ca^{+2}$) cations and ($CO^{-2}$) anionic groups. Calcite is a triangular symmetric (Fig.3.2).

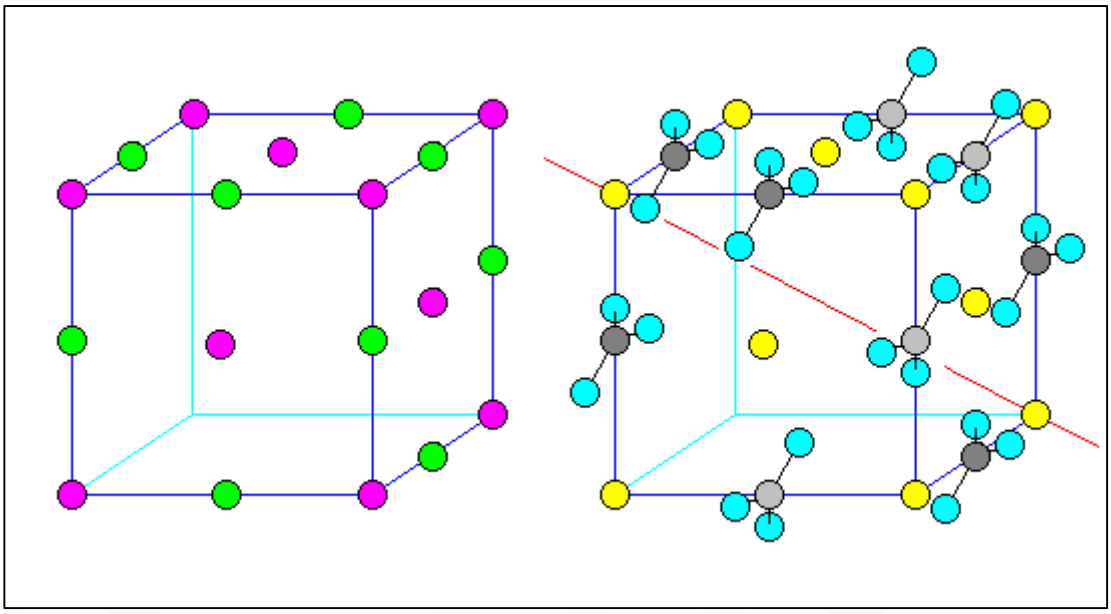

**Figure 3.2** The resemblance between NaCl and $CaCO_3$

calcite structure is not extremely sophisticated, but rather can be difficult to envision. It is often portrayed as an "altered NaCl" structure.

On the left in (Fig.3.2) represent structure of NaCl, with purple sodium atoms and green chlorine atoms (albeit both have the same atomic positioning, it barely matters). On the right in (Fig.3.2) is calcite indicating calcium in yellow, blue is oxygen, and carbon is gray. We can see that there are columns of substituting Ca and $CO^3$ units, much the same as Na and Cl interchange in halide.

Calcite is not cubic. Carbonate groups are separated by cubic symmetry in several ways. To begin with, their triple symmetry axis is aligned with a symmetry axis of the cube (in red) (Fig.3.2). Calcite has triangular crystal framework and calcite can be in different colors. Assortments of calcite in anthraconite, stain spar, iceland spar, prasochrome, aphrite, argenite e.g. Mn, Fe, Zn, Co, Ba, Sr, Pb are found as normal polluting influences in calcite. Calcite can be unsafe to wellbeing, yet there is no particular information on wellbeing threats or the harmfulness of this mineral. Be that as it may, you ought to dependably regard mineral specimens as possibly harmful and hazardous and utilize sensible safety measures when dealing with them [25].

### 3.2.2 Defects within the Crystal Structure

The alkali halides assembly comprises of a systematic positioning of alkali and halide ions, in a steady progression, rotating in each of the three bearings. Figure (3.3) demonstrates the structure of two perfect crystals.

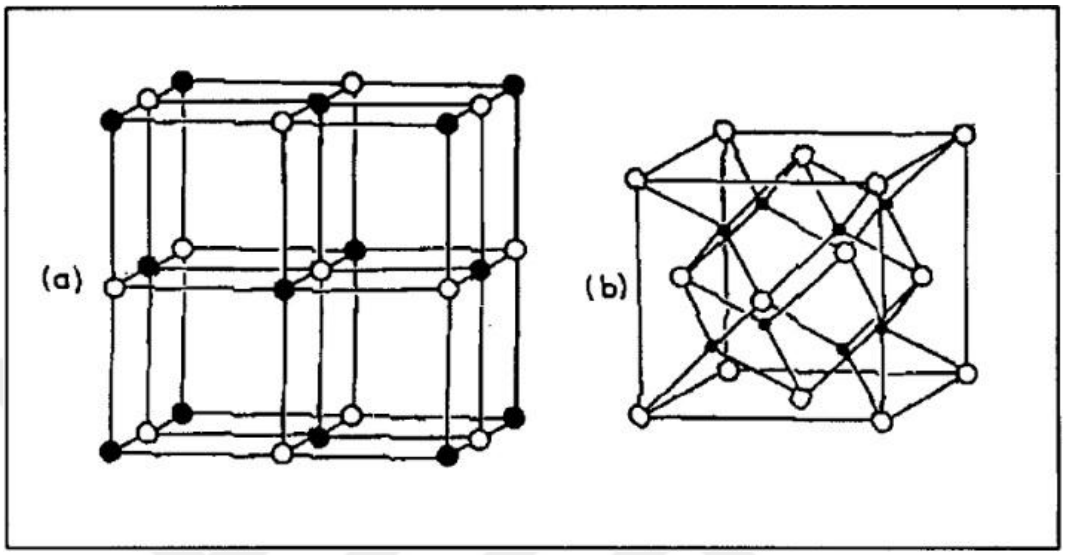


**Figure 3.3** Three-dimension assembly for the ideal crystal: (a) Structures of LiF. (●Li , ○F) ; (b) structures of $CaF_2$ (●Ca , ○F).

Despite what might be expected, a genuine crystal has imperfections which are essentially of three general sorts: (Fig. 3.4 portrays three sorts of imperfections)

1. The first type of imperfections are the inherent or indigenous deformities and they can be:

a) "Missing atoms" as Vacancies ("Schottky defects"): An empty lattice point is a variant obtained when one atoms is removed from the sites and not replaced.

b) "Interstital or Frenkel defect": It consists of (an atoms x) embedded in (crystal x) on an incorrect section of the grid.

c) "Substitutional defects": For instance, "halide ions in alkali sites".

d) Aggregates types of past deformities.

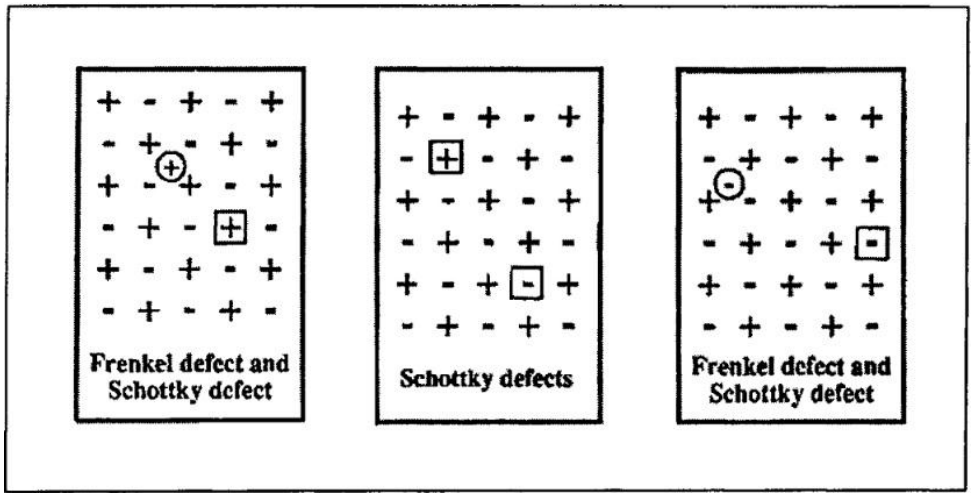


**Figure 3.4** A truly crystalline structure with characteristic defects i.e. LiF, + alkali ion (Li+), - halide ion (F-), [+] alkali ion vacancy, [-] halide ion vacancy, (+) interstitial alkali ion, (-) interstitial halide ion.

2. Second type of imperfection is extraneous or defilement flaws, similar to chemical defilement (Y) in a crystal (X), they can be:

a) "Substitutional" defilement: an atoms (Y) replaces an atom (X).

b) "Interstitials" defilement: atoms (Y) is introduced into an additional sites that does not take place with an ideal crystal.

For instance here in Fig.3.5; it demonstrates the acts of the divalent cation $Mg^{+2}$ in LiF, which replaces Li ions.

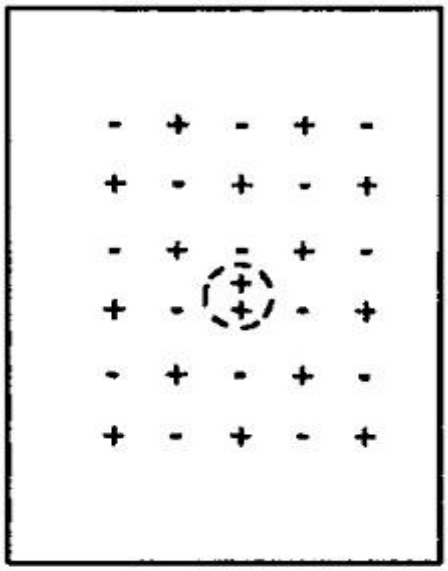

**Figure 3.5** Substitution divalent cation impurity Mg2+ in an alkali halides crystal.

To comprehend the system of substance polluting influences, the impact of a divalent particle on vacancy focus is not noticeable. As it shown in Fig. 3.6 (a): In order to make up for the pollution positive charge, one alkaline particle must be discarded. In addition, since divalent cation contamination is a local positives charges and the cationic vacancy is a local negative charge, they attracts each other's. Secure the connection as shown in figure 3.6 (b).

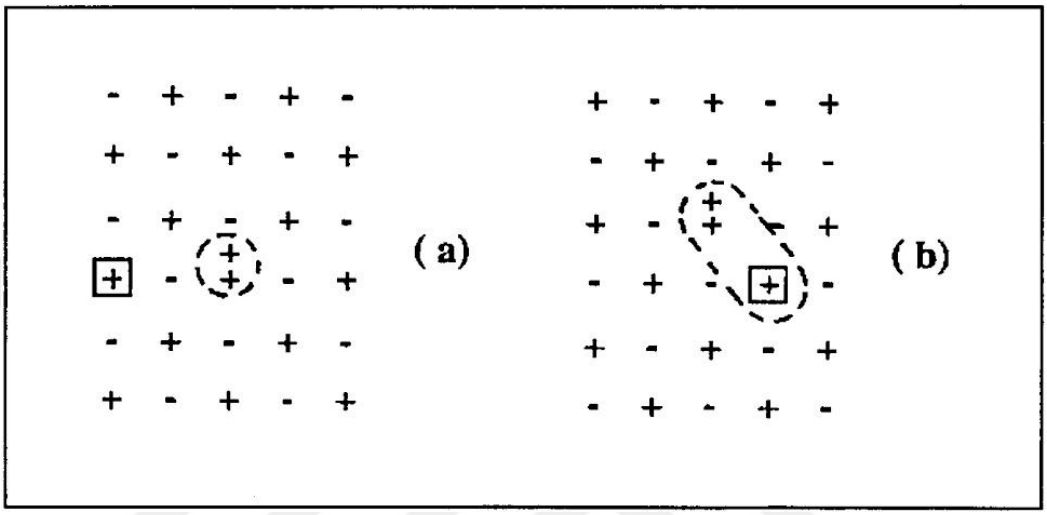


**Figure 3.6** (a) an alkali ion missing; (b) attraction of ions to form a complex.

3. Third type of imperfection is that ionizing radiations deliver additional imperfections in alkali halides.

These imperfections are called color centers, it is the absorption center, colored ionic crystals. For instance, negative ions vacancies are districts of localized positives charges on the grounds that the negative ions which typically possesses the site is missing and the negative charges of the encompassing particles are not killed. Thus, ionizing radiation allows electrons to roam within the crystal and can introduce electrons into a limited positive charge by Coulomb forces, and can be trapped in vacancies. This framework is called "F" center (Fig. 3.7).

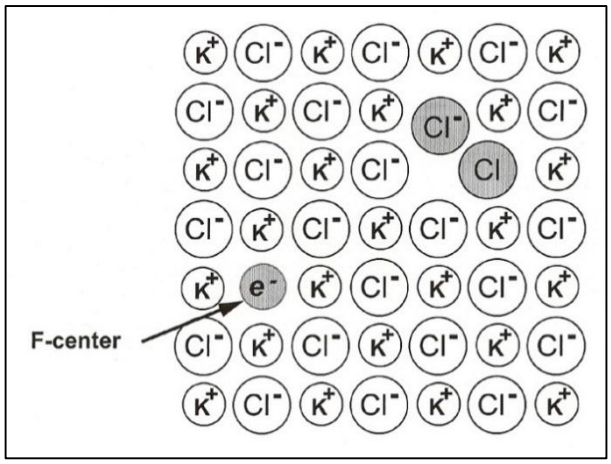


**Figure 3.7** F center in alkali halide crystal

Correspondingly, a positives ions vacancy expresses to a hole traps and this framework is called "V" focus. Different sorts of hole centers are perhaps:

- The $V_K$ focus is acquired when holes are confined by two negative particles.

- The $V_3$ focus contains unbiased halogen particles containing sites of halogen ions resulting in two halide particles trapped by two holes.

The V, $V_K$, $V_3$ imperfections are shown in Fig. 3.8.

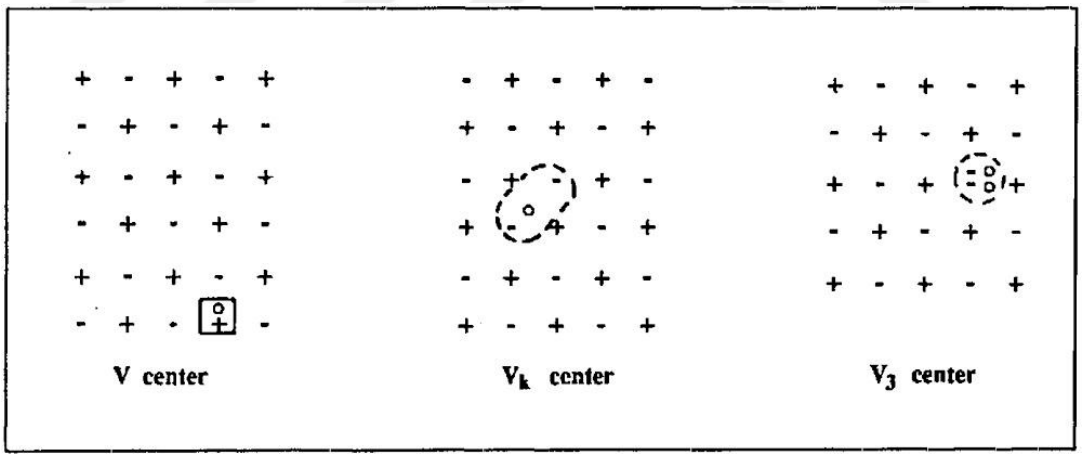


**Figure 3.8** V, $V_k$ and $V_3$ centers in a real crystal.

Its needs to layout the significance of the imperfection generation amid irradiation since high dosage levels can instigate undesirable impacts in TL materials, for the most part known as radiation damage, this is crucial in establishing and supporting a framework for Thermoluminescence dosimetry, namely, reducing impact, immersing in effects, and so on.

Therefore, the phenomenological short-term components of radiation failure in crystals are shown below.

Photons, electrons, neutrons, charged-and-uncharged motes can make imperfections by uprooting as in the barraging radiation dislodges the crystal molecules from their typical position in the grid; creating opportunities and interstitially. The quantity of deformities delivered is relative to irradiation flux and irradiation time. Be that as it may, amid a long irradiation, the quantity of imperfections delivered will progressively diminish in light of the fact that the likelihood of vacancy-interstitial recombination increases.

These defects include either a thawed crystal assembly, or diffusion or implantation at a later stage [23].

### 3.3. Theoretical Background of Thermoluminescence

Thermoluminescence comprises of a disturbance of the electronic system of insulating or semiconducting matter. Thermoluminescence is a temperature-fortified light outflow from a crystal after expulsion of stimulation. Thermoluminescence is an instance of phosphorescence that is seen under the state of consistently expanding temperature and is called glow curve [4, 5].

#### 3.3.1. Energy Bands, Electronic Transitions in Crystalline Materials and Recombination Process

A non-conductor -like an alkali crystal- can be depicted quantum-mechanically as the band sample. The conduction band is isolated from the valance band by the forbidden area. The arrangement of the Schrödinger equation for electrons subjected to an intermittently shifting potential uncovers that the permitted energies for the electrons lie just in “permitted zones”.

Thermoluminescence needs the perplexity of a system from a condition of thermodynamic symmetry, through absorption of outer energy, at a metastable state. Then the system's thermal stimuli relax and return to their symmetrical state.

Figure 3.9 shows the energy graph of a crystal with a specific deformation number between conduction band "CB" and valence band "VB". With thermal

symmetry condition T = 0 K, all incomplete levels up to the Fermi level F are possessed by electrons. Electrons and crystal lattices are thermally symmetric.

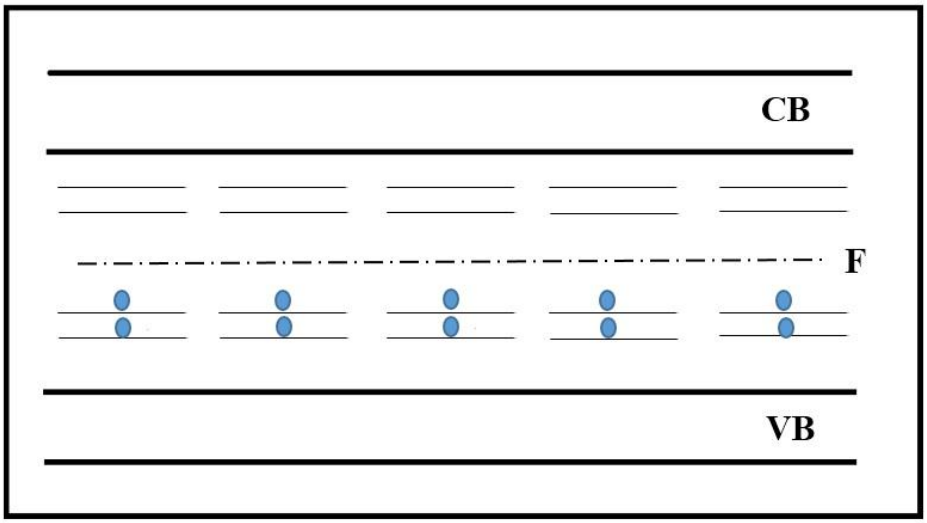


**Figure 3.9(a)** Energy maps of crystals with a specific number of flaws are interspersed among CB and VB. The open circles represent the electrons.

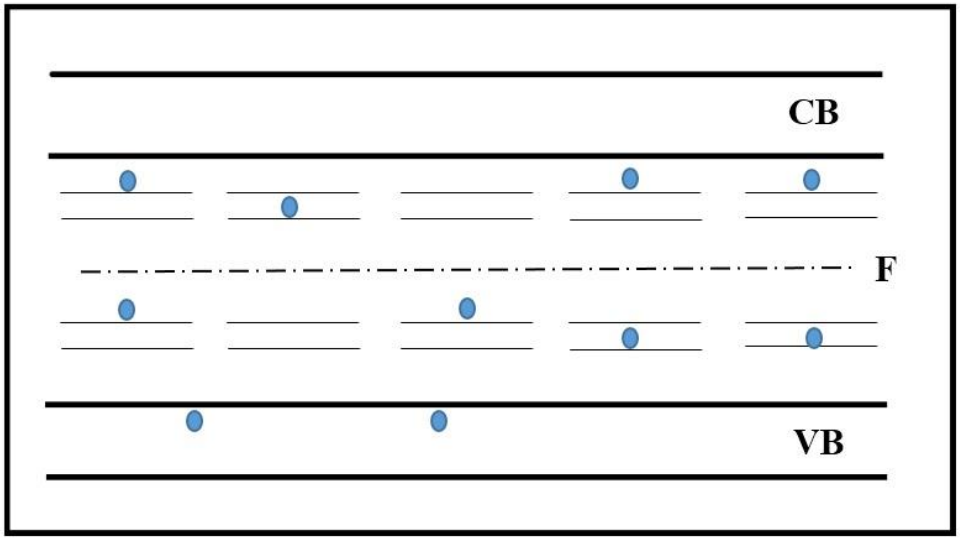


**Figure 3.9(b)** Redistribution of the caught electrons because of the illumination.

The inhabitance of each zone or band is portrayed by the state's capacity thickness, in particular N (E) = Z (E). F (E) where f (E) is the Fermi-Dirac dispersion function given by

$$\boldsymbol{F\ (E) = \frac{1}{\exp[(E-Ef)/kT]+1}} \tag{3.1}$$

In these equations, N (E) is the concentration of the involved energy states. Z (E) the density of the accessible energy states, and Ef is the Fermi level or chemical potential [9]. The energy level of the most astounding possessed orbital in a metal at the

temperature of outright zero is known as the Fermi level. The Fermi level lies at or close to the focal point of the band in some different metals. At the temperature of $0^0$K, electrons thermally over inhabit the Fermi level, and some energy levels just underneath that temperature stay abandoned. On account of a metal, the thermal inhabitants of various energy states can't be depicted as Boltzmann dispersion, however are rather given by the Fermi-Dirac dispersion [26]. The energy levels presented might be distinct, or might be dispersed relying upon the precise essence of the imperfection and of the host grid. Mainly, it is trusted that the grid flaws, defilement, intrinsic and extrinsic imperfections offer ascent to the localized energy levels (metastable state) within the forbidden gap.

The system would now be able to be disturbed by an ionizing radiation. Under irradiation, the electrons in the deformity levels, or in the valance band pick up energy, and ascend into larger amounts past the Fermi level (Fig.3.9.a). After the irradiation, a redistribution procedure happens and the energized system backpedals to symmetry (Fig.3.9.b). The time required to balance the back pacing may differ from milliseconds to several years; contingent upon the material, its imperfections and temperature [23].

All thermoluminescence phenomena are represented by the procedure of electron-hole recombination. Three unmistakable sorts of the recombination transition are conceivable. In particular, band-to-band, band-to-center and center-to-center. The band-to-band recombination might be named "direct" while recombination including localized levels, i.e. 'the levels', might be named "indirect" (Fig.3.10) [9].

Amid absorption of light in the far ultraviolet irradiation with α, β and ϒ, they compare to the freedom of an electron from the valance band into the conduction band, leaving a hole in the valance band (transition (1)). Subsequently, transition (1) compares to the procedure of ionization. The free electron in the conduction band and the free hole in the valance band roam through the crystal until the point when they wind up plainly caught in the grid imperfections. The electron might be caught by a transition to the least accessible energy level in the imperfection (transition (2)). The hole may likewise be caught in a grid deformity over the valance band (transition (3)). The caught electrons and holes might be discharged from the traps when the crystal is warmed or under the visual stimulation (transition (4) and (5)). At the point when the charge bearers are discharged to their comparing band, they are allowed one more time

to travel through the crystal and may recombine with a charge bearer of an inverse sign, either straightforwardly (transition (6)) or in a roundabout way (transition (7) and (8)) [25].

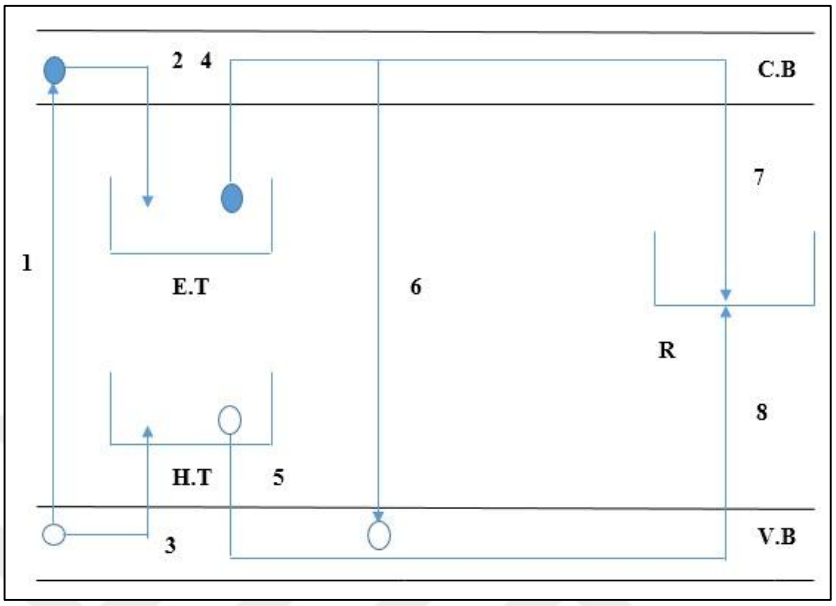


**Figure 3.10** Regular electronic transitions in a semiconductor or an insulator: (1) ionization, (2) electron trapping, (3) hole trapping, (4) electron discharge, (5) hole discharge, (6) direct recombination , (7) and (8) indirect recombination .

It ought to be noticed that there are two sorts of the luminescent focus. The first is a deformity which acknowledges a charge and then ends up noticeably total, so it stops to go about as a luminescent focus. The second is a recombination focus at which electrons and holes are wiped out. The latter might be little in numbers, yet can go about as luminescence centers as long as both electrons and holes are free. Such centers are likewise essential in photoconductivity estimations.

## 3.4 Models for Thermoluminescence

### 3.4.1 Simple Model

The free electrons and holes are made in sets and are destroyed in sets and an equivalent populace of caught holes at level R must exist. The most straightforward model for TL comprises of a single kind of electron imperfection level and a single type of electron deformity level in the forbidden gap. In the basic TL display, two levels are accepted. Those placed under the base of the conduction band and those located above the highest point of the valence band (Fig. 3.11).

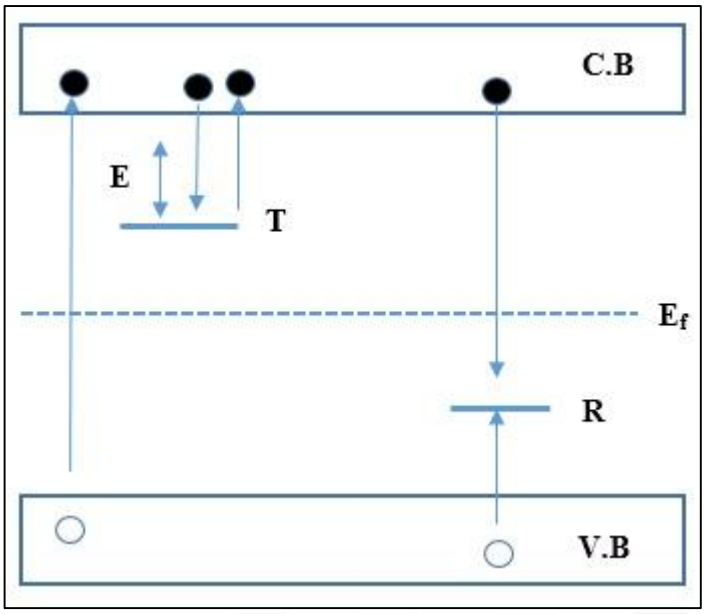


**Figure 3.11** The band model follows the basic two-layer model to demonstrate the electronic transition in the TL material.

The intensity of the thermoluminescence (IT) whenever amid the warming is corresponding to the rate of recombination of holes and electrons at level R. On the off chance that $n_h$ is the centralization of trapped holes [9].

As the temperature rises, the electrons are discharged and recombination happens lessening the convergence of trapped holes and expanding the thermoluminescence intensity. As the electron traps are dynamically exhausted, the rate of recombination declines and in this manner the thermoluminescence intensity diminishes correspondingly. The thermoluminescence is shown as a function of time. Normally in a test of this sort, temperature, as a linear function of time ,

$$\mathbf{T = T_0 + \beta t} \tag{3.2}$$

Where β is characterized as the warming rate given by $\frac{dT}{\mathrm{dT}} = \beta$

The charge bearer being thermally discharged from its trap is exponentially related to - $\frac{\mathrm{E}}{\mathrm{kT}}$ where E is the trap and the edge of the relating delocalized band. The contrast between a trap and a recombination center in light of the relative possibility of trapping and recombination prompts the likelihood that - at a given temperature - there will exist in it an imperfection level for which these transition potential outcomes are equivalent. Such a level of depth (D), would represent a boundary between the traps and the recombination center. So that a focal point of energy depth E, where

E<D, would be a trap, whilst if E>D, the site is recombination center. Because the "depth" of the trap alludes to the energy distinction between the localized level and the related the delocalized bonds (i.e. the conduction band of electrons; the valence band of holes). We have a boundary level for electrons ($D_c$), and a comparing one for holes ($D_h$). The boundary levels are appeared in Figure 3.12. At that point the scope of the temperature, over which the thermoluminescence peak shows up, is identified with the trap's depth. Actually, the position of the maximum in a thermoluminescence experiment is dictated by the blend of E and s. For given (s), one would expect that the bigger the estimations of E (i.e. the deeper the trap), the higher the temperature ($T_m$) at which the peak exists. Along these lines, a thermoluminescence experiment may - under great conditions - give appropriate data on the dissemination of trapping states in phosphor.

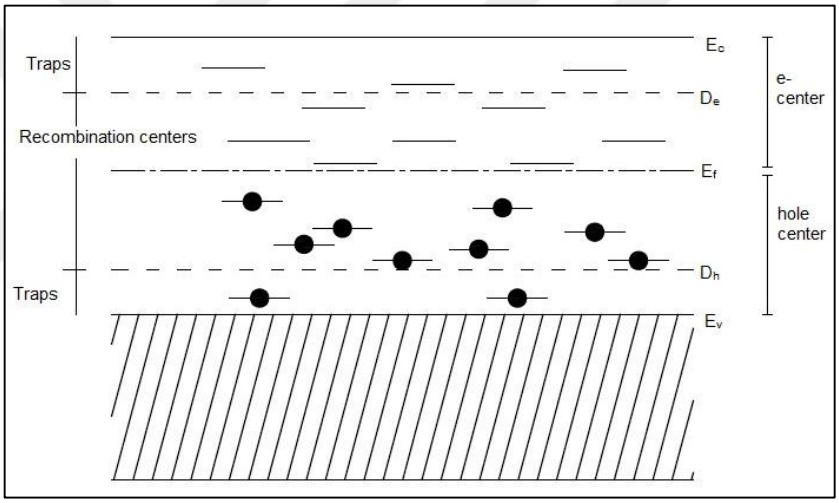


**Figure 3.12** Energy level for an insulator in balance at complete zero. The levels underneath E*f* are loaded with electrons, while those above are void.

The probability of the charge bearer being thermally discharged from its trap is greatly identified with Arrhenius equation which gives which expresses that in the time ($\tau$) an electron is trapped at temperature T [26] is

$$\tau = s^{-1} \exp\left(\frac{E}{kT}\right) \tag{3.3}$$

where “s” frequency factor. "E" is the contrast between the C B and trap position in the band gap - which is called trap depth or activation energy- and "K" is the Boltzmann's constant .

Equation can be modified as $\rho = \tau^{-1}$

$$\rho = s \exp\left(-\frac{E}{kT}\right) \quad (3.4)$$

This gives the possibility (P), per unit of time of the release of an electron from the trap. As indicated by equation (3.2), if the trap depth is - as beforehand said at the temperature of irradiation, (i.e. $T_i$, E is substantially bigger than $kT_i$) will cause the electrons delivered by irradiation and afterward trapped to stay in the trap for a drawn out stretch of time even after the evacuation of the irradiation .

The Arrhenius equation presents the idea of activation energy (E) which is regarded as an impairment of energy . This must be overcome with the final goal of achieving balance in mind.

### 3.4.2 Trap Filling Process

Following Chen McKeever Durrain (1981) the trap filling procedure might be portrayed "by the following four equations" [9]:

$$dnc/dt = ∫ - ncArnh - nc(N - n)A \quad (3.5)$$

$$dn/dt = nc(N - n)A, \quad (3.6)$$

$$dnv/dt = ∫ - nv(Nh - nh)Ah, \quad (3.7)$$

$$dn_h/dt = n_v(N_h - n_h) - n_c n_h A_r \quad (3.8)$$

The codes included are:-

- $n_c$ : is the concentration of electrons in the equilibrium band (per unit volume).
- $n_v$: is the concentration of holes in the valance band.
- n: concentration of electrons in traps.
- N: concentration of available electron traps (of depth "E" below the conduction band).
- $n_h$: concentration of holes in recombination centers.
- $N_h$: concentration of available centers.
- A: is the transition coefficient for electrons in the conduction band becoming trapped (volume/ unit time).
- $A_h$: transition coefficient for holes in the valance band becoming trapped in the hole centers.

- $A_r$: recombination transition coefficient for electrons in the conduction band with holes in centers.
- $f$: is the electron-hole generation rate (volume / unit time).

The transition coefficients to the caught cross-sections by equations of the format $A=v\sigma$, where *"v"* is the heating speed of the free transporters in conduction of valance bands, and "$\sigma$" is the cross-sections for the trap of the free charges by the trapped charges. Also, for charge balance it can be seen that:

$$n_c + n = n_v + n_h \tag{3.9}$$

### 3.4.3 Trap Emptying Process

Making an assumption that there is a single electron trap and a single hole center, the rate equations depicting the stream of charges between different energy levels and groups amid trap exhausting have been portrayed by Adirovitch (1956) [28], Hearing and Adams (1960) [29], and Halperin and Braner (1960) [30] as

$$dn_c/dt = nsexp(-E/kT) - n_c(N-n)A - n_c n_h A_r \tag{3.10}$$

$$dn/dt = n_c(N-n)A - nsexp(-E/kT) \tag{3.11}$$

$$I_{TL} = - dn_h/ dt = n_c n_h A_r \tag{3.12}$$

Where $I_{TL}$ is TL intensity (photon/sec)

In accordance with equation (3.11), $I_{TL}$ is equivalent to the rate of recombination, which is relative to the quantity of recombination centers and the quantity of free electrons. Unluckily, there is no broad systematic solution for these equations 3.10, 3.11 and 3.12. In any case, an estimated solution can be reached by making a few suppositions. Then again, numerical solutions can be found for a given arrangement of the parameters E, s, $A_r$, A, N, $N_o$, $n_o$, and $n_h$ [31-32]. These numerical arrangements are very valuable for scrutinizing the reliance of the TL curve on different parameters.

So as to acquire a systematic answer for the equations 3.10, 3.11 and 3.12, the accompanying two presumptions might be utilized:

$$n_c \ll n, \qquad dn_c/dt \ll dn/dt \tag{3.13}$$

It was likewise expected that the charge balance equation moves toward becoming:

$n_c+n = n_h$ (3.14)

Where $n_c = 0$ implies, that $n = n_h$ , $dn/dt = dn_h/dt$, and since $dn_c/dt = 0$, the conclusion from equations 3.10-3.12 is:

$$I = - \frac{dn_h}{dt} = \frac{nsexp\left(-\frac{E}{kT}\right)}{1+\frac{(N-n)\,A}{nA_r}} \quad (3.15)$$

### 3.5 Thermoluminescence of Kinetic Analysis

#### 3.5.1 First-Order Kinetic

I(t) (in equation 3.15) can't be explained systematically without extra rearranging suppositions. Randall and Wilkins [33] accepted unimportant re-entrapment amid the warming stage , i.e. they expected m A ≫( N - n )Ar. Under presumption, it can be composed as

$$I(t) = - \frac{dn}{dt} = sn \exp\{- \frac{E}{kT}\} \quad (3.16)$$

This characteristic equation is the charge transport in the grid as a primary procedure and the emission peak occurring in this equation is called the primary luminescence peak . To understand the unique equation (3.16) as a component of time,

$$I(t) = - \frac{dn}{dt} = n_0 s \exp\{- \frac{E}{kT}\}\exp\{-s \int_0^t \exp\{- \frac{E}{kT(t')}\}dt'\} \quad (3.17)$$

Where "$n_0$" number of electrons captured in time equal to zero (t=0). In general, the temperature rises in chronological order, by

$$T(t) = T_0 + \beta t \quad (3.18)$$

β as the heating rate, $T_0$ represent the temperature when t=0. This gives the strength for the function of temperature, to be

$$I(t) = -\frac{1}{\beta}\frac{dn}{dt} = n_0 \frac{s}{\beta} \exp\left\{-\frac{E}{kT}\right\} exp\{-\frac{s}{\beta}\int_{T_0}^{T} exp\{-\frac{E}{kT'}\}dT'\} \quad (3.20)$$

This is the outstanding "Randal-Wilkins" first-order articulation for single glow peak. The asymmetric symbol on the high temperature sideways is broader on the low temperature sideways thn on the high temperature side. On the first rise of the glow peak (that mean in the low-temperature part), the intensity is taken control of by the first exponential (exp (- E / k T)). Along these lines, in the event that "I" is

sketched as function ( 1/ T), the straight line is normal with the first rise in temperature and extends with slope "- E / K ", the calculation of the activation energy E, can be easily found.

The features of "Randall-Wilkins" equation are outlined in figure 3.13. In Fig.3.13.(a), it is indicated how 1(T) changes if $n_0$ change as $n_0 = 0.25\ m^{-3}$ - $n_0 = 2^{m-3}$ when E =1 eV , $s=1.0x10^{12}s^{-1}$ , β=1 K/s are still steady, it may be noticed that the temperature for the peak's maximum ($T_m$) remains settled. This is normal for all first-order thermoluminescence curves. The maximum expression is obtained by dI/dt = 0 (or slightly less demand from d1 nI (T) / dt = 0).In this case we can conclude that

$$\frac{\beta E}{kT_m^2} = s \exp\{-\frac{E}{kT_m}\} \tag{3.20}$$

In this equation $n_0$ doesn't show up, which demonstrates that $T_m$ doesn't rely upon $n_0$. It can be additionally observed from Fig.3.13 (a) that not just the peak height is at the most extreme degree, however, all points in the curve is relative to $n_0$. In dosimetric applications, $n_0$ is a basic meaningful parameter. This parameter is the absorbed dose. It is easy to see that the range under the glow peak is equal to $n_0$, so since

$$\int_0^\infty I(t)dt = -\int_0^\infty \frac{dn}{dt}dt = -\int_{n_0}^{n_\infty} dn = n_0 - n_\infty \tag{3.21}$$

And $n_\infty$ equalto zero when t→∞. In Fig.3.13 (b) "the activation energy E" varies from "0.8 to 1.2" eV. As "E" expands, as the height and width decrease, the peak moves to a higher temperature; keeping the range (i.e.) fixed.

Comparative changes may be seen as "s" is fluctuated (Fig.3.13(c)), yet now at the inverse path: as "s" expands, the peak moves to bring down temperature s by an expansion in the altitude and reduce the width. Fig.3.13 (d), show the heating rate had fluctuated. As "β" expands, peak moves to high temperature s while the altitude diminishes, and the curve width increments similarly as on account of the reduction of "s". This is normal, whereas "s" & "β" appear as "s/ β" in Equation (3.19). Note that the four parameters are worth it; "E" the activation energy, frequency factor "s" are the primary physical parameters. Those parameters are called "trapping parameters" and are resolved by trapping center attributes. The other two parameters can be selected by the experimenter by selecting a specific dose " $n_0$ " and reading the mark at a specific heating rate "β". Examining another TL material in this manner will

investigate the behavior of the glow peak from changes in absorbed dose and heating rate.

The assessment of equation (3.19) is obstructed by the way that the fundamental at the right hand is not rudimentary on account of straight warming. Chen [34] shows how it can be approximated by asymptotic arrangement . For executable applications, it is useful to describe the glow peak to parameters that are easy to decide tentatively , especially up to the "maximum" peak intensity and the maximum "Tm" temperature. Kitis and Al. [35]. It has been shown that equation (3.19) can be approximated accurately to:

$$I(T) = I_m \, exp[1 + \frac{E}{kT}\frac{T-T_m}{T_m} - \frac{T^2}{T_m^2} \, exp\{\frac{E}{kT}\frac{T-T_m}{T_m}\}(1-\Delta) - \Delta_m] \quad (3.22)$$

As of late, Pagonis and Al. [36] have demonstrated that a weibull distribution, which is a standout amongst the most regularly utilized distributions in unwavering quality designing as a result of the many shapes it achieves for different values of b (slopes) [37], the function likewise precisely portrays the first-order thermoluminescence curve. These statements are suitable for the purpose of "peak fitting".

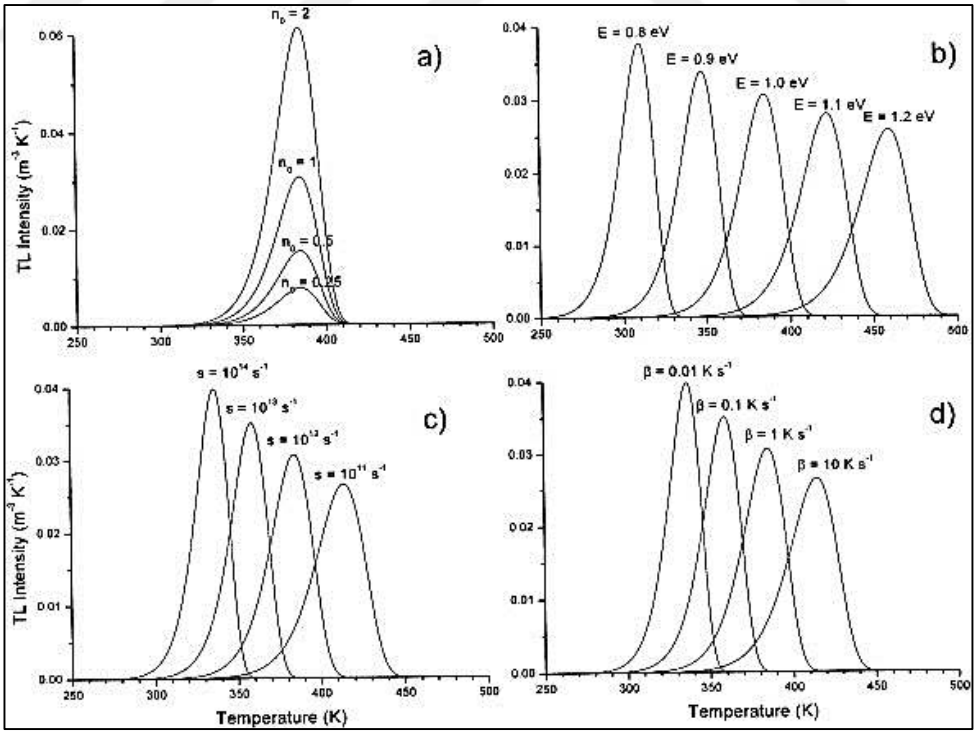


**Figure 3.13** Properties of Randall and Wilkins 1st order TL equation, and it demonstrates: (a) Variety by "n0", which is the grouping of the trapped charge transporters after irradiation,(b) the variety with "E" which is the activation energy,(c) the variety with "s" which is the escape frequency, (d) the variety with β which is the

heating rate. Parameter's values: n0=1 m-3 E=1 eV; s=1x 1012 s-1, β=1 K/s; in which one parameter is shifted while the others are kept fixed.

### 3.5.2 The Second-order Kinetics

Garlick and Gibson [38] thought about how possible it is that re-entrapment for the most part take control, i.e. $mA \ll (N-n)A_r$. Moreover, they expected that the trap is a long way from immersion, i.e. $N \gg n$ and $n = m$. With these suspicions in the picture, equation (3.15) progresses toward becoming

$$I(t) = -\frac{dn}{dt} = s\frac{A}{NA_r}\, n^2 exp\,\{-\frac{E}{kT}\} \tag{3.23}$$

Now $\frac{dn}{dt}$ is corresponding to $n^2$, which implies 2nd order reaction . With the extra supposition of equivalent possibilities in "recombination and" re-entrapment, "$A=A_r$"; in this manner, the consolidation of equation (3.15) moves toward becoming

$$I(t) = \frac{n_0^2}{N}\frac{s}{\beta}\, \exp\{-\frac{E}{kT}\}|1 + \frac{n_0 s}{N\beta}\int_{T_0}^{T} exp\left\{-\frac{E}{kT'}\right\} dT'|^{-2} \tag{3.24}$$

This is "Garlick-Gibson" TL equation for second order energy. The focus of this curve is that it is nearly symmetric and the curve at half the height at high temperature is somewhat wider than half of the low temperature". This is unmistakably comprehended in the event that we considered the way that in 2nd order reaction, critical convergences of discharged electrons are re-caught before they even recombine. Therefore, it is possible to postpone luminous luminescence and diffuse luminescence over a wider temperature range. The potential focus "$n_0$" Here not only is shown as a multiplicative constant as in the case of the first order, different dose level changes change the state of the entire curve. This is shown in Fig.3.14 (a), and we can see that $T_m$ diminishes as $n_0$ increments. So it can be inferred [39] the change in temperature can be approximated to "$T_1 - T_2 \approx T_1 - T_2 \frac{k}{E} 1n\ f$"

"$T_1$" the temperature of the intensity "$I_m$" at specific dose, "$T_2$" is the temperature of most extreme intensity at a higher dose "$f$". "With the given parameter estimations" of Fig.3.14 (a), the shift is 25K while " E=1 eV ", "$T_1$=400 K ", and the absorbed dosage is expanded by a factor of 1000 - which is anything but difficult to temporarily acknowledge- and a "temperature shift" of 77K is unsurprising. From equation (3.25) it additionally demonstrates that if that dose expands, the trap will be shallower and the peak's movement will be bigger. Figure 3.14 (b) shows the change

in secondary peak size and position as a function of " E", while in Fig.3.14 (c) “s” is the function of “ s /N ” , and Fig.3.14 (d) “s” is the function of the heating rate . Although the area under the curve corresponds to the initial concentration $n_0$, the height of the peak is not particularly related to the area of the peak despite the fact that the deviation is small.

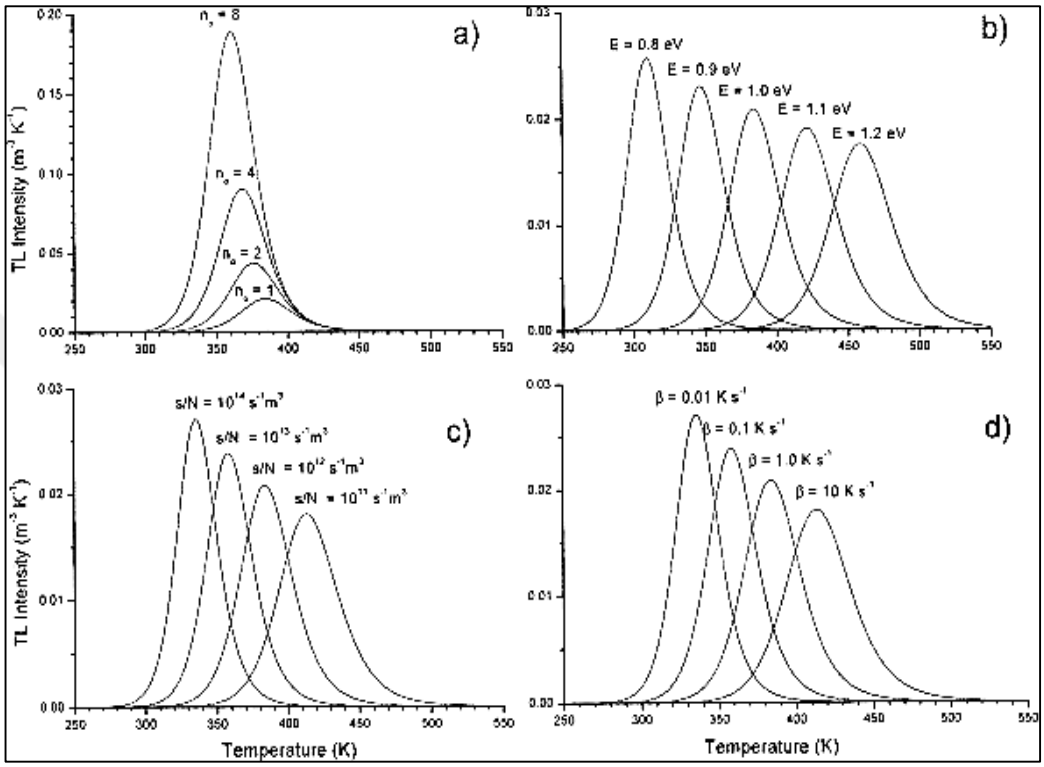


**Figure 3.14** Properties of Garlick and Gibson’s 2nd order TL equation.

Note the similarity between the first-order case and the second-order case in the expression "ruling the temperature’s reliance in the initial rise” exp (- E/kT). Here, you can also apply the "initial rise method" that guarantees the depth of the trap.

Additionally for 2nd order kinetics, glow peak's shape in equation (3.24) can be approximated. Given that the most extreme peak's intensity is "$I_m$" and the greatest peak’s temperature is "$T_m$" [35]. Thus, the equation after approximation moves toward becoming

$$I(T) = 4I_m \exp\left(\frac{E}{kT}\frac{T-T_m}{T_m}\right) \times \left[\frac{T^2}{T_m^2}(1-\Delta)\exp\left\{\frac{E}{kT}\frac{T-T_m}{T_m}\right\} + 1 + \Delta_m\right]^{-2} \quad (3.26)$$

$P.S.\ \Delta$ *and* $\Delta_m$ *have the same meanings as in equation* (3.26)

### 3.5.3 General-Order Kinetics

The first and second order types of the thermoluminescence equation were obtained from the utilization of particular and streamlining suppositions . Be that as it may, when these improving presumptions don't hold together, The TL peak will not be suitable for primary and secondary kinetics.

May and Partridge [40] utilized a brief articulation for this situation for general-order TL energy, particularly

$$\text{I(t)} = -\frac{dn}{dt} = n^b s' \exp\{-\frac{E}{kT}\} \tag{3.27}$$

Where " s '" has the measurement of "$m^{3\,(b-1)}\ s^{-1}$" and " b " is characterized as the general-order parameter which doesn't have to be 1 or 2 Joining of equation (2.19) if b ≠1 results in

$$\text{I(T)} = \frac{s'}{\beta}\, n_0 \exp\left\{-\frac{E}{kT}\right\} [1 + (b-1)\frac{s'}{\beta}\int_{T_0}^{T} exp\left\{-\frac{E}{kT'}\right\} dT']^{\frac{-b}{(b-1)}} \tag{3.28}$$

Where (s') =$sn_o^{b-1}$ with unit $s^{-1}$. Equation (3.28) incorporates the second-order case (b=2) and decreases to equation (3.19) where b→1. It ought to be noticed that as indicated by equation (3.27), the measurement of (s') ought to be $m^{3\,(b-1)}\ s^{-1}$. This means that thee measurement results change in the order of "b", which makes physical decoding difficult. The case of a general-order is still valuable because the intermediate case can be managed, and when b → 1 and b → 2 they easily go to first and second order (see figure 3.15).

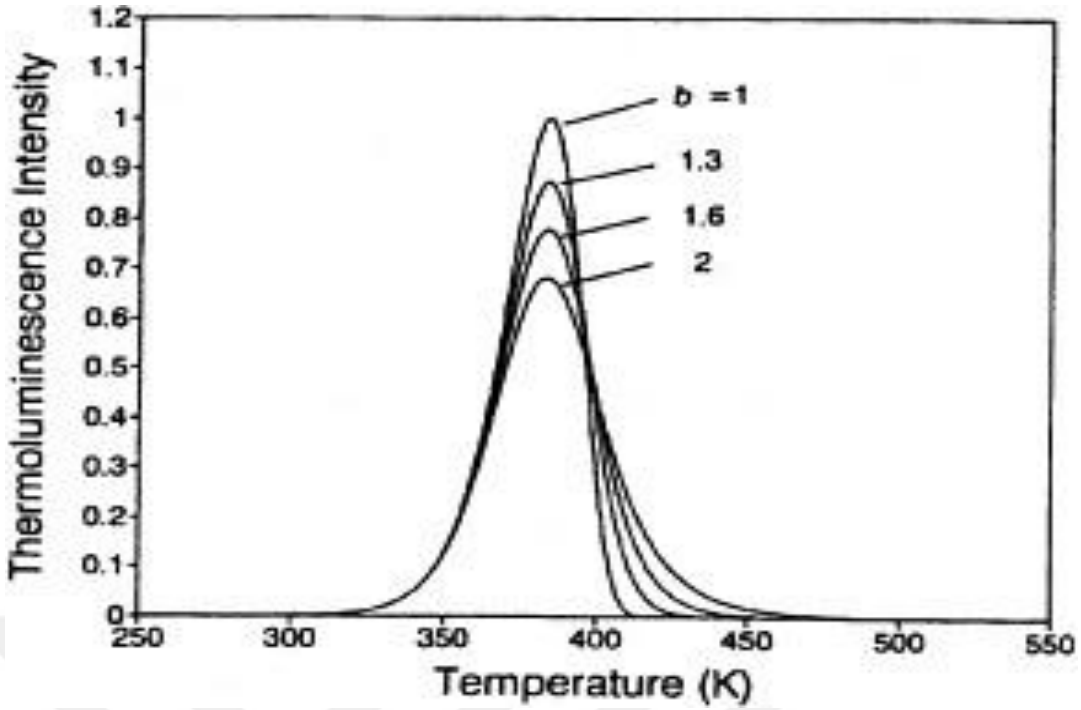


**Figure 3. 15** Comparison of first-order (b=1), second-order (b=2) and intermediate-order (b=1.3 and 1.6) TL peaks, with E=1 eV, s=1* $10^{12}$ $s^{-1}$, n0=N=1 $m^{-3}$ and β=1 K/sec [35].

# CHAPTER 4

# THERMOLUMINESCENCE ANALYSIS

## 4.1 Trapping Parameter Determination method

Many methods found to estimate the trapping parameters from the glow curve [33 , 41 and 42]. Methods such as initial rise, variable heating rate, isothermal decay, and peak shape are suitable for situations where the glow peaks are separated from each other.

If the peaks are combined, tow ultimately methods to calculate the parameters, these methods are partial thermal cleaning method, and computer glow curve deconvolution program. Partial cleaning method, overwhelmingly, is insufficient to detach the peak perfectly without disturbance, thus, the computer glow curve deconvolution program befit to estimate trapping parameters from TL glow curves in these days [43].

### 4.1.1 Peak Shape Method

Grossweiner [44] was sophisticated the first peak shape method, then Chen [42] amend Halpevin and Braners equation [45] for determine E values.

Chen [46] used numerical approximations to obtain an expression to estimate E values. Chen methods is advantageous for a wide range of energies between 0.1 eV – 2.0 eV and pre-exponential factors between $10^5$ $sec^{-1}$ and $10^{13}$ $sec^{-1}$. Moreover, this method needs no knowledge of kinetics order, because it is directly found from the peak slope.

This method depends on the shape of TL peak, exactly like to Lushchik [47] and Halberin Braner method [46]. For simplicity, the parameters involved in a well resolved peaks are here reported in fig.4.1.

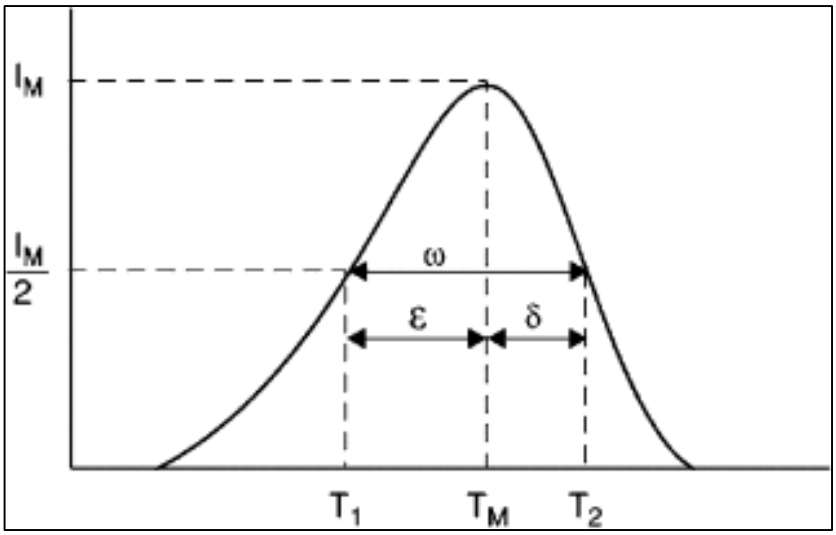


**Figure 4.1** Parameters characterizing of single peak.

The order of kinetic "b" is determined by the shape parameter. Chen obtained that "$\mu_g$" is not affected by E changes, but it will with order kinetics b changes. As it shown, In the case of linear heating, μg range for b = 2 from 0.42 at b = 1 to 0.52.

To extrapolating and interpolating the constants that come in the equations in the first and second order , Chen provides general expression epitomize all the sooner expressions.

$$E\alpha = C\alpha \left[\frac{KK_m^2}{\alpha}\right] + b\alpha\,(2T_m) \tag{4.1}$$

Where α is τ,σ or w . The values of $C_\alpha$ and $b_\alpha$ are shown below:

$$C\tau = 1.5 + 3.0\,(\mu_g + 0.42) \qquad b\tau = 1.58 + 4.2\,(\mu_g + 4.42)$$

$$C\sigma = 0.97 + 7.3\,(\mu_g + 4.42) \qquad b\sigma = 0 \tag{4.2}$$

$$Cw = 2.52 + 10.2\,(\mu_g + 4.42) \qquad bw = 1$$

With

$\mu_g = 0.42$ for 1st order

$\mu_g = 0.52$ for 2nd order

Chen [48] draw a graph of $\mu_g$ for values of b . The range of $\mu_g$ from " 0.36 to 0.55 " while b was between "0.7 to 2.5". This graph can be used for estimate "b" from measured $\mu_g$ (see Fig. 4.2).

Balarin [49] Suggest a graph giving the kinetics order as a function of $Y = \frac{\sigma}{\tau}$ (Fig. 4.3).

If activation energies are obtained, easily, the frequency factor can be calculated by using the following equation.

$$s = \left(\frac{\beta}{T_m^2}\right)\left(\frac{E}{K}\right)\frac{1}{1+(b-1)\left(\frac{2KTm}{E}\right)}\exp\left(\frac{E}{KT_m}\right) \tag{4.3}$$

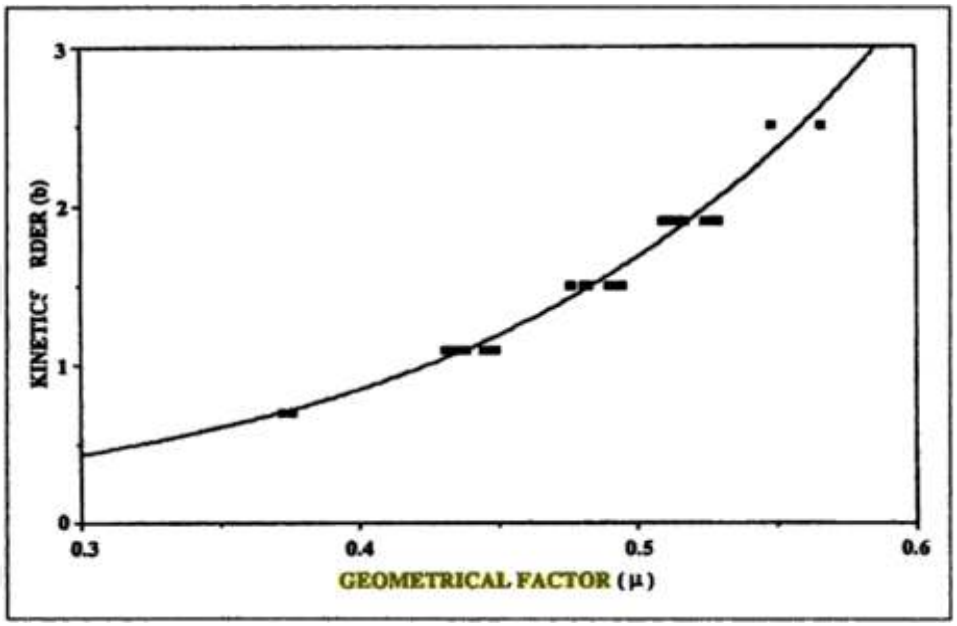


**Figure 4.2** Curve of kinetic order b as a function of geometric factor μg = σ/w [5].

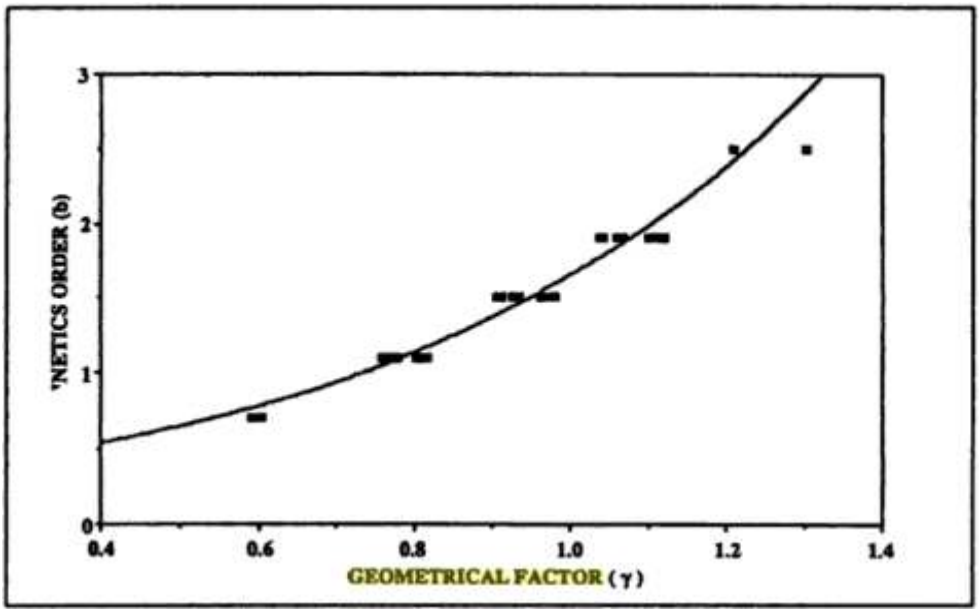


**Figure 4.3** Curve of kinetic order b as a function of geometric factor $_{\gamma}$ = σ/τ [5].

### 4.1.2 Isothermal Decay Method

The isothermal decay method completely changed the capture parameter analysis. TL sample temperature is constant and luminescence is recorded as a function of time. Before time, Galick and Gibson [38] were explain this method for the first-order kinetics. The following equations is obtained for the 1st order kinetics in case of T constant, and $n_o$ is the initial value of "n"

$$I_{(m)} = -C\,\frac{dn}{dt} = -C\,\frac{n_o}{\tau}\,exp\left(\frac{-t}{\tau}\right) \tag{4.4}$$

$$\tau = s^{-1}\exp\left(\frac{E}{KT}\right) \tag{4.5}$$

The equation from the previous constant temperature "T", the emission of light will be exponentially decay with time t, the graph of "$\ln(I)$" and t will appears as a straight line with a slope= $s\exp\left(\frac{-E}{KT}\right)$ .

Let thee initial integral light b "$S_o$, $S_{ti}$" be the integral light at time $t_i$":

$$S_o = n_o$$

$$S_{t1} = n_1 = n_o \exp(-p\,t_1) \tag{4.6}$$

$$S_{tn} = n_n = n_o \exp(-p\,t_n) \tag{4.7}$$

At T = constant

Making ratio

$$m_i = -S\exp\left(-\frac{E}{K\,T_i}\right) \tag{4.8}$$

Which

$$\ln mi = -S\exp\left(-\frac{E}{K\,t_i}\right) \tag{4.9}$$

Thus, the sketch of $\ln(m)$ and $^1/_T$ exhibit straight line of slope $-\,{}^E/_K$ and $\ln(-S)$ on the ordinate axis.

When experiments are carried out at different constant storage temperature s like " $T_1$ and $T_2$", the toe slopes "$m_1$ and $m_2$":

$$\ln\left(\frac{m_1}{m_2}\right) = \frac{E}{K}\left(\frac{1}{T_2} - \frac{1}{T_1}\right) \tag{4.10}$$

The last equation allows to calculate E

$$E = \frac{K}{\left(\frac{1}{T_2} - \frac{1}{T_1}\right)} \ln\left(\frac{m_1}{m_2}\right) \quad (4.11)$$

Frequency factor s substitution of the E value in equation 4.8.

The isothermal decay method is not useful for higher order kinetics. Kathuria and Sunta [50] were suggest a method from isothermal decay method of Thermoluminescence to calculate the order of kinetics, it was in 1979. In this method, if the decaying intensity at a constant temperature is held, the sketch between $I^{(1/b-1)}$ and t gives a straight line, while a suitable value of b is picked. Thence, several values of b are attempt to pick correct one that gives a straight line.

### 4.1.3 CGCD Method

To estimate the trapping parameters from TL glow curve, this method is very important method and easy to use. "CGCD" method is suitable more than other experimental methods, It can be used in the overlap peak of the glow curve, because there is no need to return to heat treatment.

This program was developed at the Nuclear Research Institute in Delft, The Netherlands [51]. The program eligible to deconvoluting up to nine glow peaks from glow curve in one time. Two models are used in the computer program , in one model, the glow curve approximates the first order kinetics , and it given by expression

$$I_{(T)} = n_o s \exp\left(-\frac{E}{kT}\right) \exp\left[\left(\frac{skT^2}{\beta E}\right) * \left(0.9920 - 1.620\frac{kT}{E_n}\right)\right] \quad (4.12)$$

While the second model, the glow curve approximates the general TL kinetics by using expressions

$$I_{(T)} = n_o s \exp\left(-\frac{E}{kT}\right)\left[1 + \left(-\frac{(b-1)s}{\beta}\frac{kT^2}{E}\exp\left(-\frac{E}{kT}\right) * \left(0.9920 - 1.620\frac{kT}{E_\alpha}\right)\right)\right]^{\frac{b}{b-1}} \quad (4.13)$$

$n_o(m^{-3})$ is the density of the trapped electrons at t=0, $s(s^{-1})$ is the frequency factor for the first order and the pre-exponential factor for the general-order, $E(eV)$ the activation energy, $T(K)$ absolute temperature, $k(eVK^{-1})$ Boltzmann's constant, $\beta({}^{o}Cs^{-1})$ heating rate and b the kinetic order.

The sum of the total peak and background contributions can result in a composite glow curve formula as shown below

$$I_{(T)} = \sum_{i0=1}^{n} I_{(T)} + \alpha + b\exp(T) \qquad (4.14)$$

Where $I_{(T)}$ is the fitted overall glow curve, a allows for electronic noise contribution to the planchete and dosimeters infrared contribution to the background.

From equation (4.14), last square minimization procedure and F.O.M "Figure of Merit" were used to assessor the fitting result as good or not. i.e.

$$F.O.M = \sum_{i=1}^{n} \frac{|N_i(T) - I(T)|}{A} = \sum_{i=1}^{n} \frac{|\Delta N_i|}{A} \qquad 4.15$$

Where "$N_i(T)$" is the i-th experimental points (total n = 200 data points), $I(T)$ is the i-th "fitted points, and $A$ is the integrated area of the fitted glow curve.

From many experiences [52 – 53], it can be said that if the values of the "FOM are between 0.0% and 2.5% the fit is good, 2.5 % and 3.5 % the fit is fair, and > 3.5 % it is bade fit".

In order to obtain a graphical representation of the agreement between the experiment and the fitted glow curve , the computer program also plots this function,

$$X(T) = \frac{N_i(T) - I_i(T)}{\sqrt{I_i(T)}} \qquad 4.16$$

This is a normal variable with expected values 0 and $\sigma = 1$, where $\sigma^2$ (T) = $I_i$ (T)

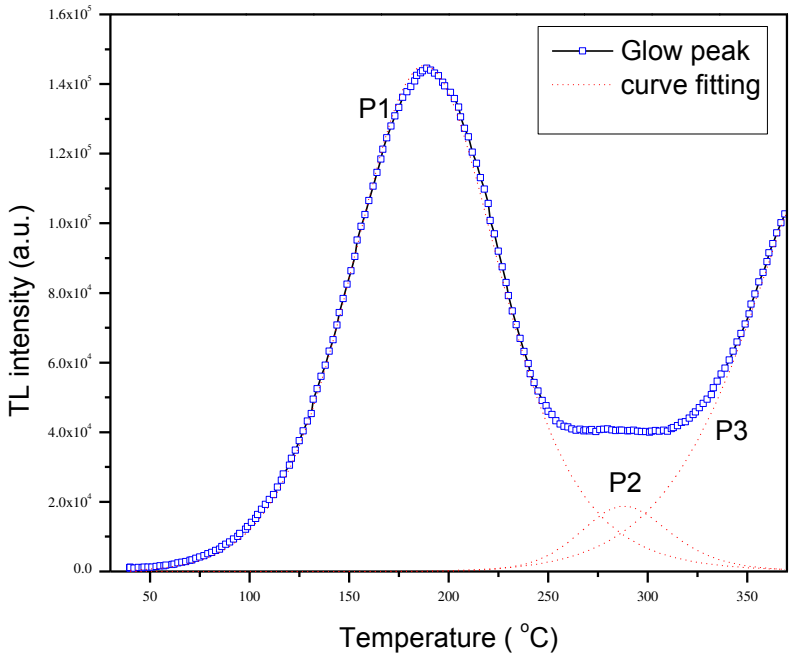


**Figure 4. 4** CGCD method fitted curve.

### 4.1.4 Initial Rise Method

Initial rise method is very easy and suitable to apply for estimate activation energy E of a single TL peak. This method based upon assume that at low temperature end of the peak, all the pertinent occupancies of the state, the recombination center, the trap, and in some case, other interactive state can be considered as being approximately constant.

The of the estimated intensity as a function of temperature in this region is, therefore, very close to exponential, thus

$$I_{(T)} = C \exp\left(-\frac{E}{kT}\right) \tag{4.17}$$

Where the constant C contain all dependencies on the other parameters and occupancies, E is the activation energy (eV), k is the Boltzmann's constant ($eV/K^{-1}$) and T is the temperature (K).

By plotting $\ln(I)$ with $^1/_T$ a linear sketch will be obtained with a slope equal to $-{}^E/_k$ . Therefore, E is possible to calculate without knowledge about the frequency factor s from means of equation

$$E = -k \frac{d(\ln I)}{d(\ln {}^1/_T)} \tag{4.18}$$

If E value was obtained, frequency factor s will be calculate from the equation

$$\frac{\beta E}{kT_m} = s \exp\left(-\frac{E}{kT_m}\right) \tag{4.19}$$

$T_m$ is the temperature at the maximum intensity. This method useful only if the glow peak is well defined and clearly separated from the other peaks.

### 4.1.5 Heating Rate Method

Various heating rate is one of the important methods for determine activation energies. The peak temperature will be different when the sample heating with various linear heating rates as $\beta_1$ and $\beta_2$. Equation (4.19) can be used for calculating E values, by putting each heating rates and dividing the equation for $\beta_1$ and $T_{m1}$ by the equation for $\beta_2$ and $T_{m2}$ and rearrange , will obtain equation (4.20)

$$E = k\,\frac{T_{m1}T_{m2}}{T_{m1}-T_{m2}}\,\ln\left[\left(\frac{\beta_1}{\beta_2}\right)\left(\frac{T_{m2}}{T_{m1}}\right)^2\right] \tag{4.20}$$

In heating rates method, the main feature is need only data to be possessed at the maximum of glow peak ($T_M$, $I_m$) , In the case of large peaks surrounded by smaller satellites , the glow curve can be determined with reasonable accuracy. Moreover, the calculation of E will not affected by problems of thermal quenching, like the initial rise method.

By using various heating rates for the first order kinetic, an expression is obtain, as shown below:

$$\ln\left(\frac{T_m^2}{\beta}\right) = \left(\frac{E}{k}\right)\left(\frac{1}{T_m}\right) + constant \tag{4.21}$$

If a sketch between $\ln\left(\frac{T_m}{\beta}\right)$ and $\left(\frac{1}{T_m}\right)$ is plotted, a straight line must be obtain with a slope $E/_k$, then E is found.

This method of various heating rates is can be used for general order kinetics which involved the second order case. For general order case, can be plotting $\ln\left[I_m^{b-1}\left(T_m^2/_\beta\right)^b\right]$ versus $1/_{T_m}$, its slope equal to $E/_k$.

# CHAPTER 5

# EXPERIMENTAL PROCEDURE

The materials equipment and experimental procedures utilized in this work are described below.

## 5.1 Materials

The samples used in this study were calcite crystals collected from DUHOK city north of Iraq.

## 5.2 Equipment

### 5.2.1 Radiation source and irradiation procedure

The samples were irradiated at room temperature immediately after quenching. Calcite crystals were irradiated with $^{90}$Sr-$^{90}$Y β-source. The activity of the beta source is about 100 mCi. On March 10, 1994 by the manufacturer was calibration. The recommended working life-time is about 15 years. Stronium-90 emit high energy beta particles from their daughter products $^{90}$Sr-0.546 MeV together with $^{90}$Y, β-2.27 MeV. Beta radiation is absorbed by air, so its intensity declines with distance much more rapidly than inverse square law calculations would indicate. The maximum range of Y-90 beat particles in air approximately 9 meter . The irradiation equipment is an addition to the 9010 Optical Dating System, purchased from Little More Scientific Engineering, England [54]. The irradiation source devices connected to PC computer using a serial RS-232 port. Our irradiation source gives 0.04 Gy per second. Calcite crystals were irradiated to various dose levels 2.4Gy to 2.3 kGy.

### 5.2.2 TL Analyzer and TL Measurement

The glow curve measurements for calcite crystals were made using a HARSHAW TLD system 3500 Manual TL Reader [55]. It economically provides high reliability. The technical architecture of the system includes both the Reader and a DOS-based IBM-compatible computer connected through a standard RS-232 serials

communication port to control the 3500 Reader. The basic block diagram of Reader is shown in figure 5.1. All functions are divided between the reader and the specialized TLD. Shell software runs on the PC computer. All data storage, instrument control, and operator inputs are performed on the PC. Signal acquisition and conditioning are performed in the reader. In this way, each glow curve can be analyzed using a best-fit computer program based on a Marquardt algorithm minization procedure, associated to first order and general order kinetic expressions. The program resolves the individual peak present in the curve, giving the best values for the different peak parameters. The instrument includes a sample change drawer for inserting and removing the TLD elements. The reader uses contact heating with a closed loop feedback system that produce adjustable linearly ramped temperature from 1 $^{o}$C to 50 $^{o}$C per second accurate to within ± 1 $^{o}$C to 400 $^{o}$C in the standard reader.

The Time Profile (TTP) is user defined in three segment: Preheat, acquire, and anneal, each with independent time (Pre-heat anneal: adjustable 0 to 1000 sec, linear ramp: adjustable from 1 $^{o}$C to 50 $^{o}$C per second, Post-read anneal: 0 to 1000 sec) and temperature (Pre-read anneal: room temperature to 200 $^{o}$C, Post-read anneal: up to 400 $^{o}$C). The typical time temperature profile is shown in figure 5.2. To improve the accuracy of low-exposure reading and extend planchet life, the 3500 provides for nitrogen to flow around the planchet . By eliminating oxygen in the planchet area, the nitrogen flow eliminates the unwanted oxygen-induced TL signal. Nitrogen is also routed through the photo-multiplier tube (PMT) chamber to eliminate moisture caused by condensation. Glow curves were measured using a platinum planchet at a linear heating rate of 1 $^{o}$C/sec . The time duration between irradiation and necessary TL operation was always kept constant at about 1 min, expect for the storage time experiment. For the variable heating rates were varied from 1 to 15 $^{o}$C/sec.

Each crystal was read twice and the second readout is considered to be background of reader plus crystal and was subtracted from the first one and all of the analyses have been carried out after subtractions.

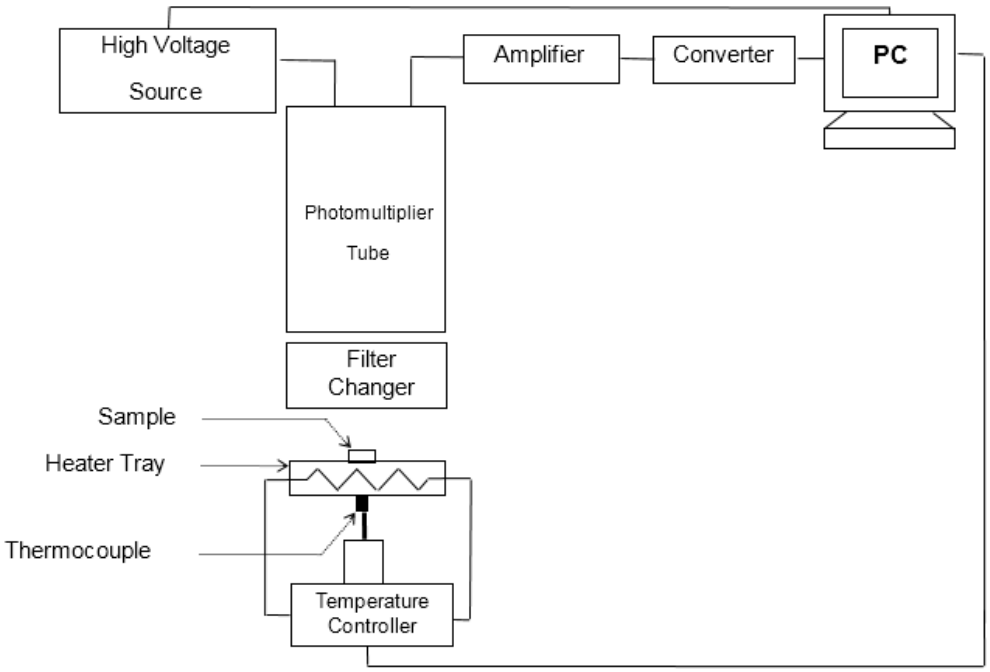


**Figure 5.1** Basic block diagram of TL reader

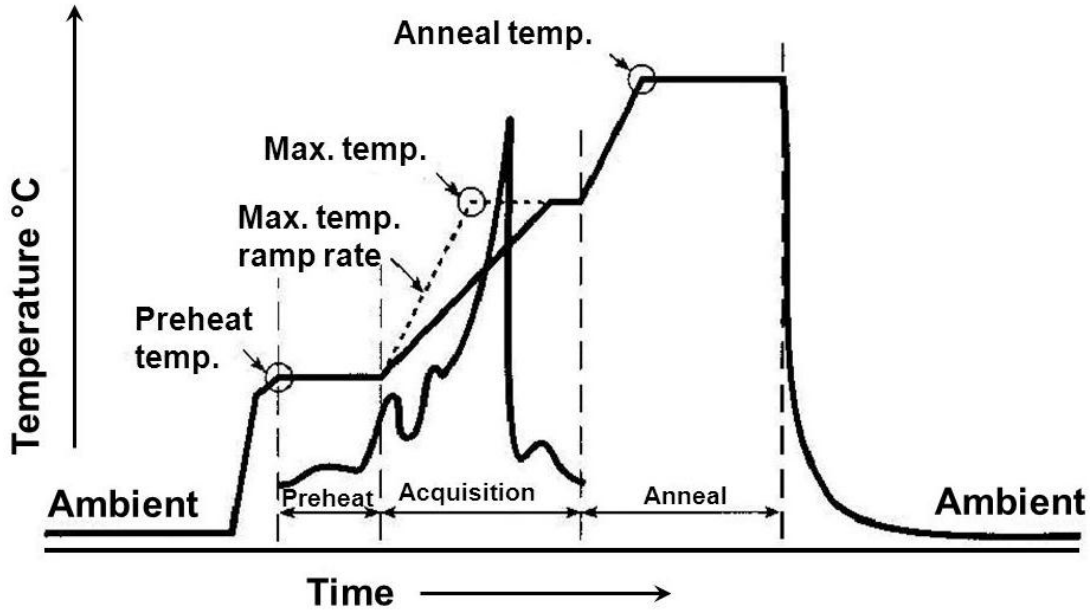


**Figure 5.2** Typical time temperature profile (TTP)

### 5.3 Experimental Procedure for Calcite

Calcite sample which was in soild state collected from nort of Iraq / dohuk city from Aqra mount.

The samle was irradiated at room temperature e with beta rays from a calibrated $^{90}Sr$-$^{90}Y$. The irradiated samples were read with a Harshaw QS3500 manual reader interfaced with a PC under $N_2$ atmosphere, where the TL signal was studied and analyzed. The method used to determine the kinetic parameters is peak shape method.

# CHAPTER 6

# EXPERIMENTAL RESULTS

## 6.1 Results and Discussion for Calcite

In order to estimate $E_\alpha$ value and s, it must have a previous knowledge about b and number of glow curve precisely [56]. TL measurements for the samples were done in air at the temperature range from 30 to 400 $^0$C, and we investigated three main glow peak in this study. The AD method applied first in this study to configure knowledge about b for glow peaks separated from each other. The sample was irradiated with different doses of 2.4 Gy up to 2.3 kGy and the effect of dose dependence on the peak position was investigated.

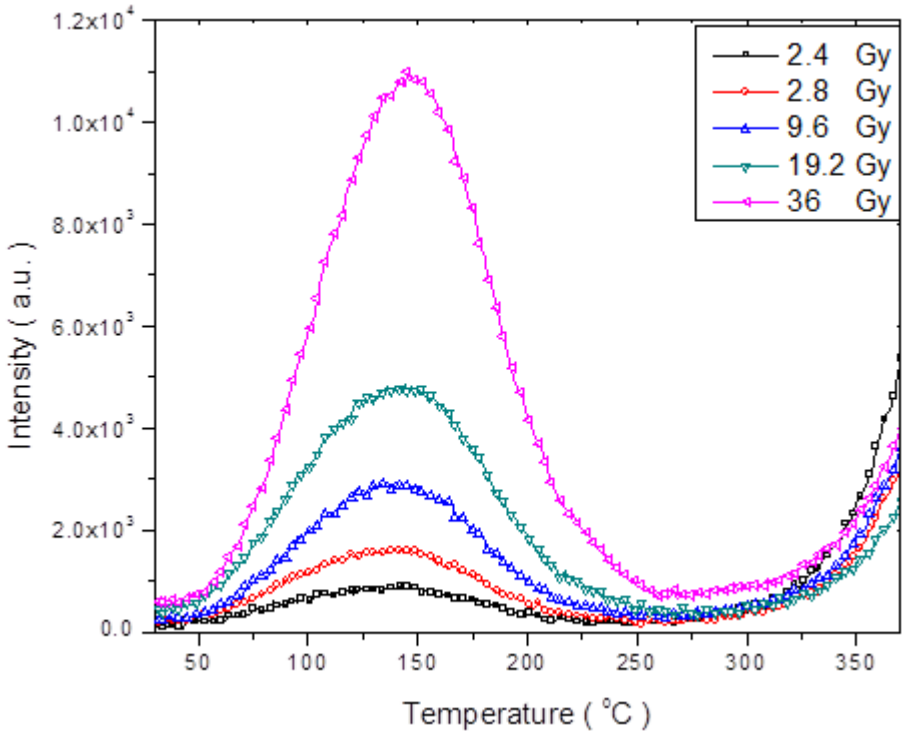


**Figure 6.1 A** The glow curve of calcite samples was measured after various doses from 2.4 to 36 Gy ($\beta = 1\ ^0C\ s^{-1}$).

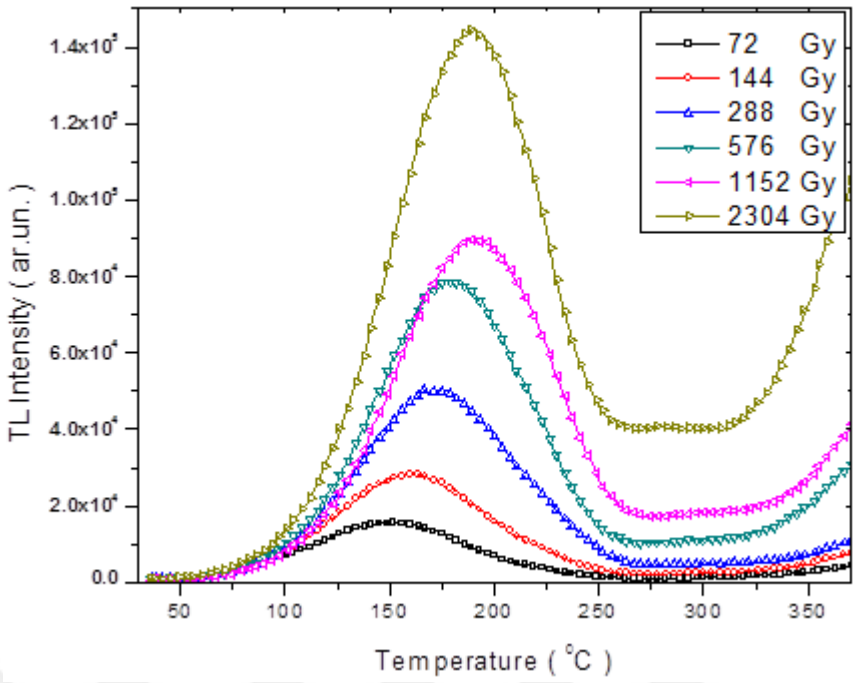


**Figure 6.2B** The glow curve of calcite samples was measured after various doses from 72 to 2.3 kGy ($\beta = 1\ ^0C\ s^{-1}$).

This is the easiest method for the first order kinetics. Figure 6.1show instance of glow curve irradiated at different dose. According to thermoluminescence theory, assume that the peak temperature not affected by experimental parameters when the heating rate is constant, except for limited experimental error differences. However, as $b \neq 1$ and below the trap fullness point {$n_0$ (trap electron concentration)> Nt (trap concentration)}, the peak temperature moves to the low temperature side as the dose level increases. From Figure 6.1. We see a slight change in the peak temperature for all doses.

In this study, the variable heating rate method was applied to obtain the trapping parameters of glow peaks at 189 and 280 $^0$C. Heating rates vary from 1 to 15 ° C / sec. Fig 6.2 show the many glow curve of VHR method. The main feature in VHR method is only (Im and $T_m$) data is required to be taken at the maximum of TL peak.

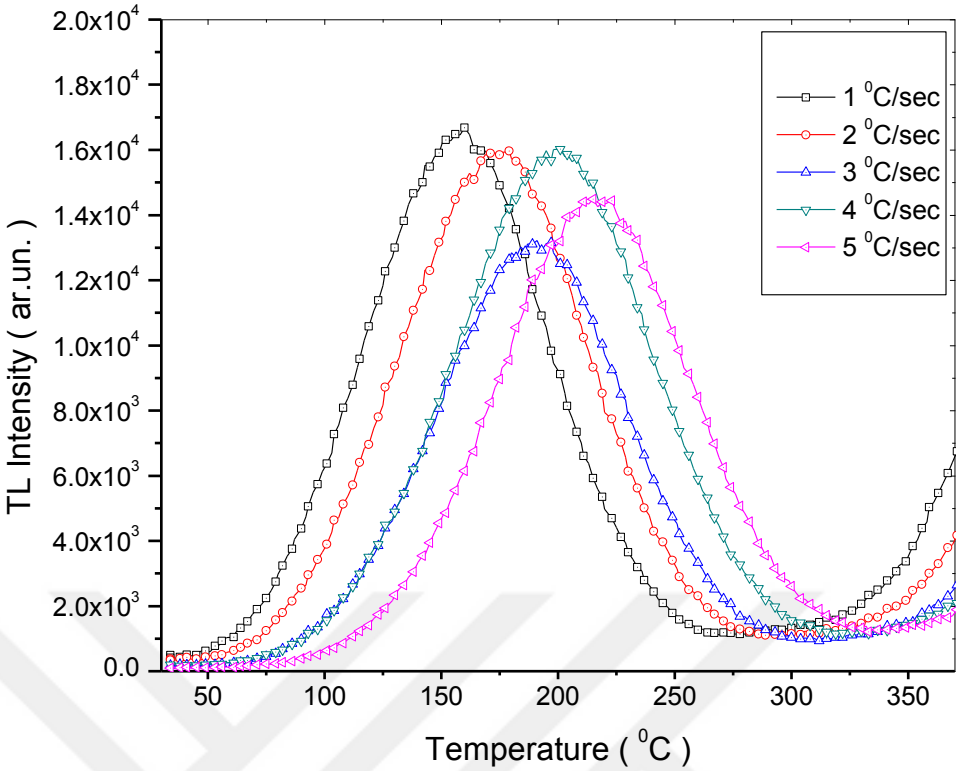


**Figure 6.2A** Glow curves at various heating rates from 1 to 5 C/sec after irradiation of calcite samples to dose level 36 Gy.

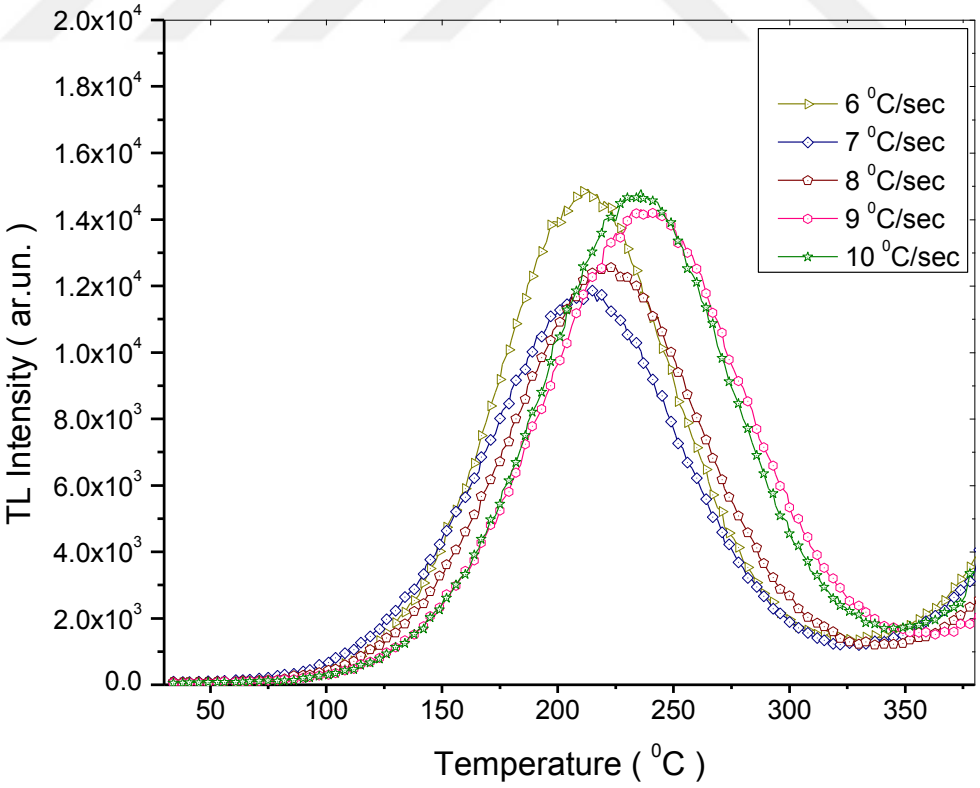


**Figure 6.2B** Glow curves at various heating rates from 6 to 10 C/sec after irradiation of calcite samples to dose level 36 Gy.

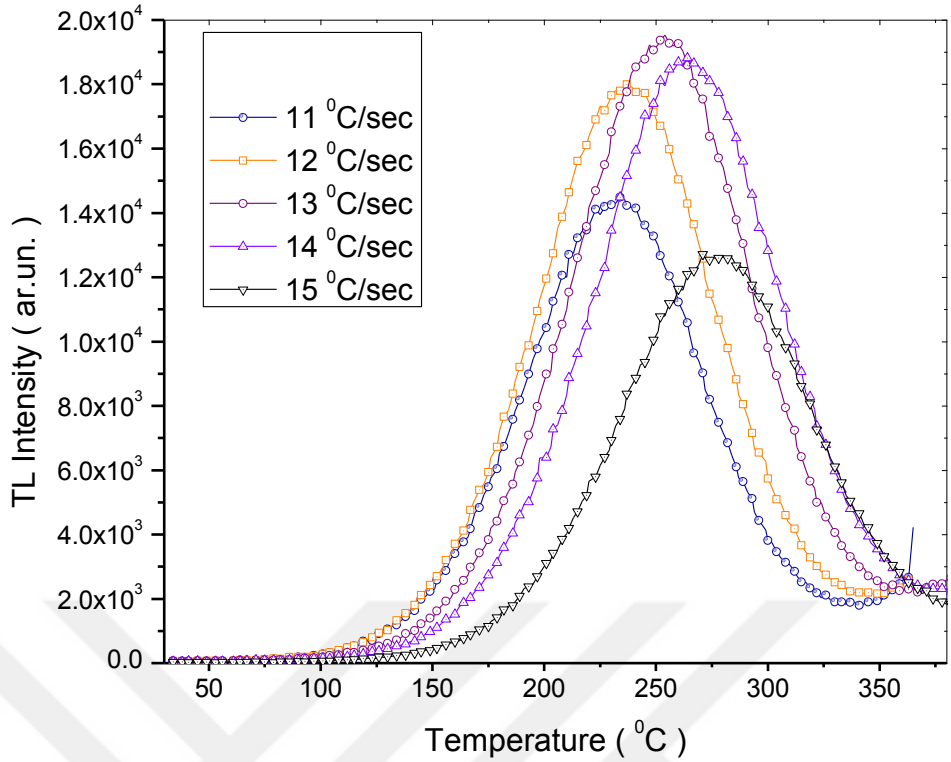


**Figure 6.2C** Glow curves at various heating rates from 11 to 15 C/sec after irradiation of calcite samples to dose level 36 Gy.

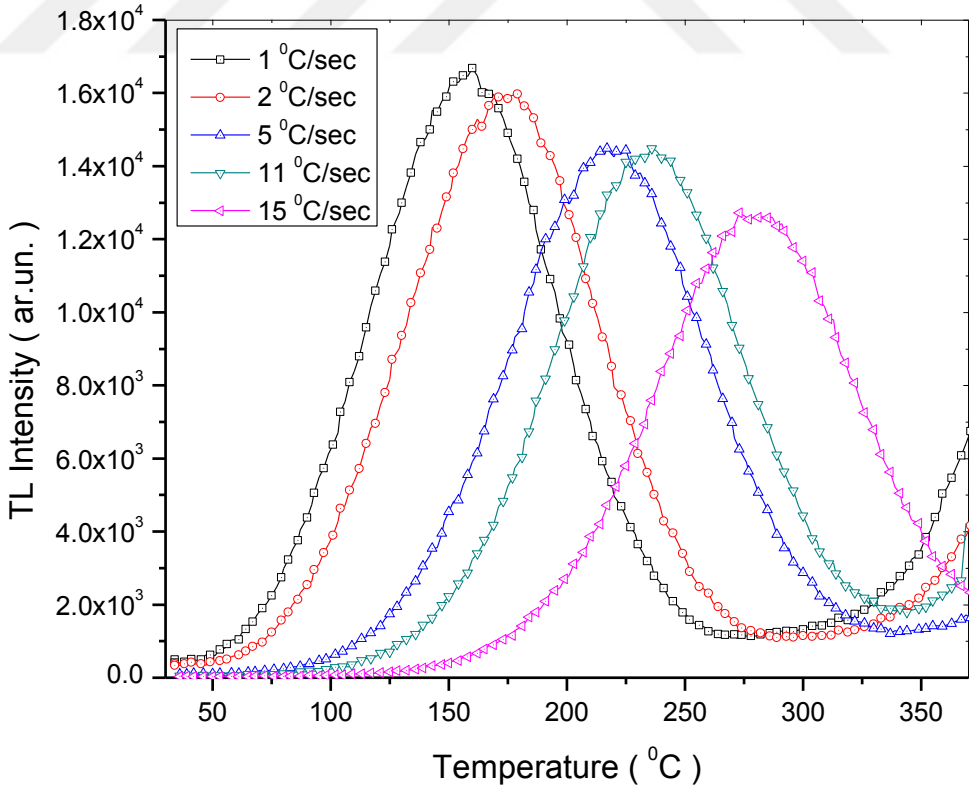


**Figure 6.3** Some of selected glow curve of calcite sample measured at various heating rates as 1, 2, 4,5,11 and 15 0C/sec.

As previously known, according to the thermoluminescence theory in VHR method if the heating rate increases, the intensity of glow peak will decreases and peak temperature shifting towards high degrees . Figure 6.3 show that for some selected curve for heating rates 1, 2, 4, 5, 11 and 15 $^0$C / sec.

In this study, data for VHR method show an error occur in the intensity and peak temperature s position, that they are not gone as the theory states. To show this error, some of glow curve selected in figure 6.4 for heating rates = 1,2,3,4 and 5 $^0$C/sec, these curves will be used to complete calculations.

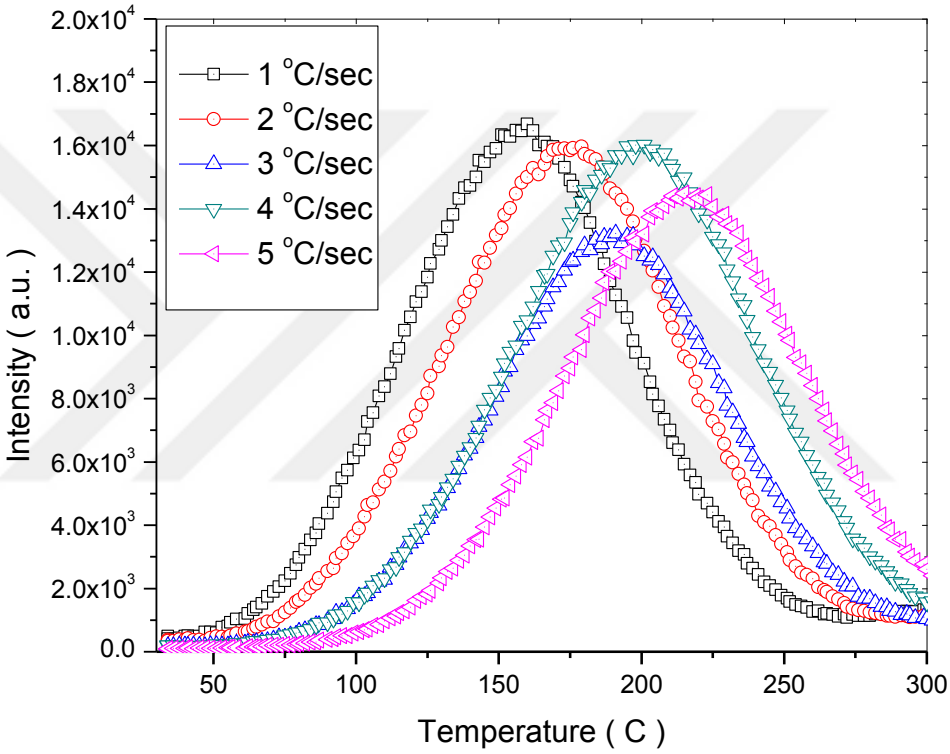


**Figure 6.4** Selected glow curves of calcite sample after irradiated at dose level 36 Gy at different heating rates = 1,2,3,4 and 5 °C /sec.

Another important issue to consider in order to avoid major errors in the calculation of kinetic parameters by the VHR method is the temperature lag (TLA) between the heating element and the thermoluminescent sample during TL reading by a contact-heated reader . To avoid this problem, Kitis and Tuyn recently proposed an easy way to correct the TLA and use the flow equation to determine the exact peak temperature for different heating rates:

$$T_m^j = T_m^i - C \ln\left(\beta_i / \beta_j\right)$$

Where $T_m^j and T_m^i$ are the highest temperature s of the glow peak of the heating rates βi and βj, respectively, C is the constant calculated initially from two low heating rates, where TLA can be considered as negligible. Preferably be the selected heating rate to calculate C value are less than 10 °C / sec. On the other hand, since the TLD reader used herein does not tolerate a low heating rate of less than 10 °C./s, a constant C is calculated using two intermediate values 1 and 2 °C/s heating rate and the maximum Peak position of value TLA and experiment point compensation. As can be seen from Figure 6.5, the relate between heating rate and maximum peak temperature when plotting $T_m$ against β it gone approximately as a straight line.

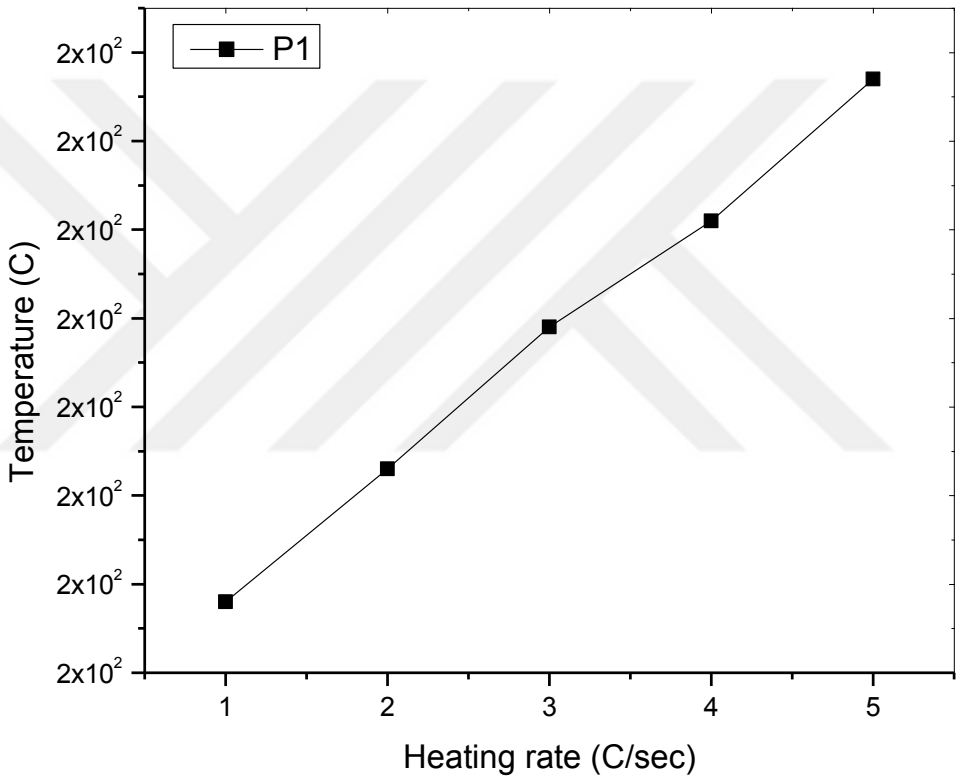


**Figure 6.5** Variable heating rate plots for peak 1 and peak 2.

From Fig 6.6, w , σ , and τ were calculated to estimate μg value according to Mazumdar peak shape method, it found μg = 0.473 , then the kinetic order b = 1.4 , now it easy to calculate activation energy values, it given in table 6.1.

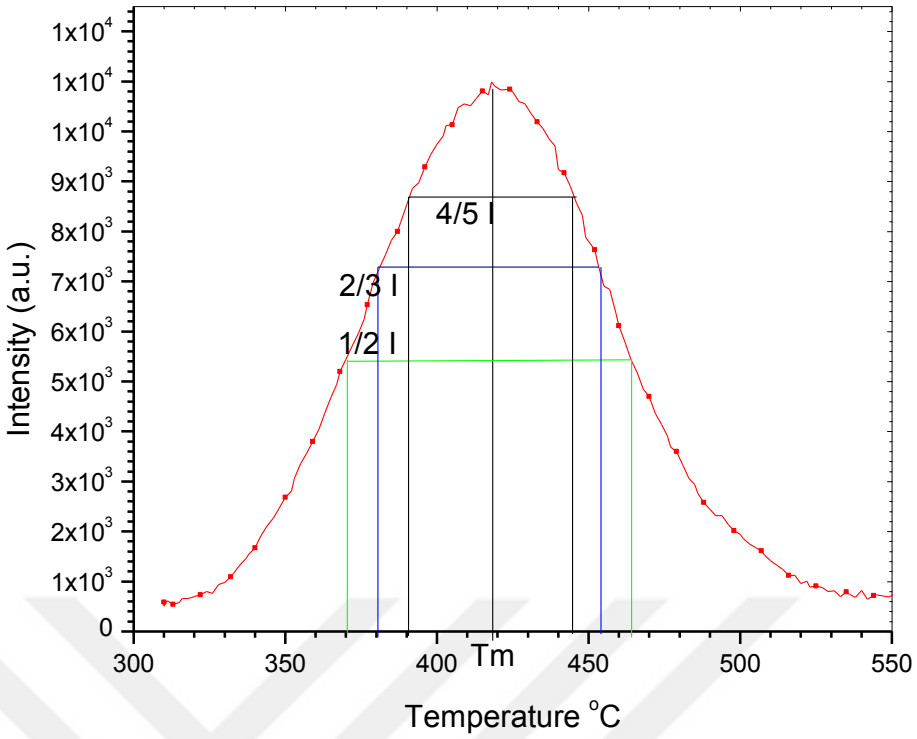


**Figure 6.6** Mzumdar peak shape method graph.

**Table 6.1** E values calculated by Mazumdar peak shape method

| | | | |
|---|---|---|---|
| **1/2 Im** | **E $\tau$ =** | **3.31E-01** | **(eV)** |
| | **E $\delta$ =** | **3.02E-01** | **(eV)** |
| | **E $\omega$ =** | **3.18E-01** | **(eV)** |
| **2/3 Im** | **E $\tau$ =** | **3.00E-01** | **(eV)** |
| | **E $\delta$ =** | **3.07E-01** | **(eV)** |
| | **E $\omega$ =** | **3.05E-01** | **(eV)** |
| **4/5 Im** | **E $\tau$ =** | **3.02E-01** | **(eV)** |
| | **E $\delta$ =** | **3.41E-01** | **(eV)** |
| | **E $\omega$ =** | **3.13E-01** | **(eV)** |

**Table 6.2** E and ln(s) values calculated by Chen & Mazumder peak shape and CGCD methods.

| CHEN Peak Shape Method | | Mazumdar Peak Shape Method | | | | | | CGCD method | |
|---|---|---|---|---|---|---|---|---|---|
| | | 1/2 $I_m$ Ratio | | 2/3 $I_m$ Ratio | | 4/5 $I_m$ Ratio | | | |
| E (eV) | ln(s) $s^{-1}$ | E (eV) | ln(s) $s^{-1}$ | E (eV) | ln(s) $s^{-1}$ | E (eV) | ln(s) $s^{-1}$ | E (eV) | ln(s) $s^{-1}$ |
| **0.417** | **9.09** | **0.317** | **8.78** | **0.306** | **8.50** | **0.308** | **8.54** | **0.5** | **12** |

The symmetry factor by Chen peak shape method is calculated and found μg = 0.473. This value mean general kinetic order (b=1.4). The activation energies were calculated by this methods.

Stored signal in room temperature and its stability one of the significant factor in many usage such as geological and archeological dating. if the decay of the stored signal can be cognizable when it stored at RT, the relation of the TL transmission and the exposition radiation may be cancelled, which may be transmitted sometime before being read out. If not measured directly, especially in archaeological applications, the extent to which the TL signal decays over a long period of time is difficult. The calcite glow curve measured at the end of the planned storage period is shown in Figure 6.6. It can be seen from the figure that the intensity of the low temperature peak 1 rapidly increases while the storage time of the high temperature peak 2 at room temperature is not sufficiently affected.

After the storage at room temperature for 3 weeks, peak1 was completely disappeared from the glow curves, but peak 2 did not change during this period. After 1 hour of storage at room temperature, peak 1 was dropped to 50 % of its Basic value and reached 12 % after 24 hours of storage during this period.

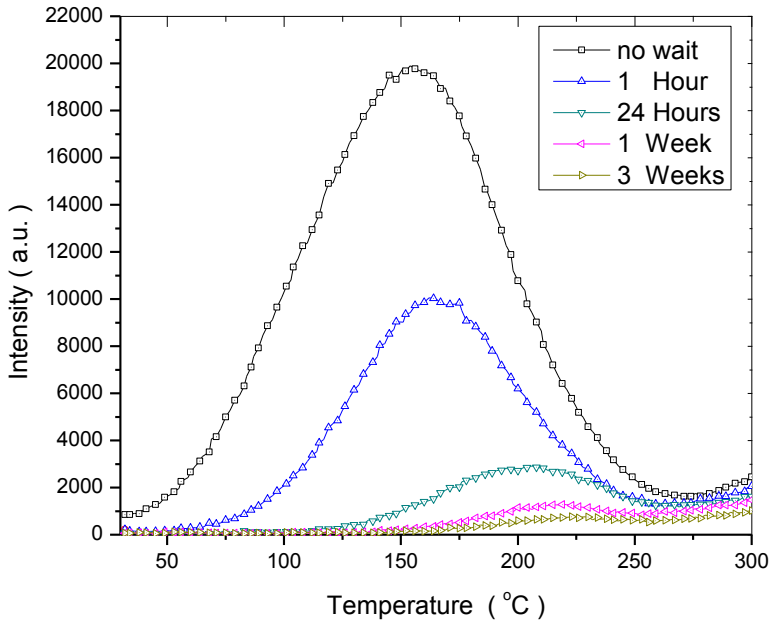


**Figure 6.7** Glow curve for calcite sample after storage in the darkbox at RT, then recorded.

The dose response was also studied by the peak elevation method of all components of calcite emission curves. As shown in Figure 6.7, all data on the dose response is displayed on a logarithmic scale. As shown in Figure 6.7, it is clear that the dose responses of all components correspond to a similar scheme. In addition, the linear slope decreases with increasing temperature, and the average peak 1 dose response is above peak 2.

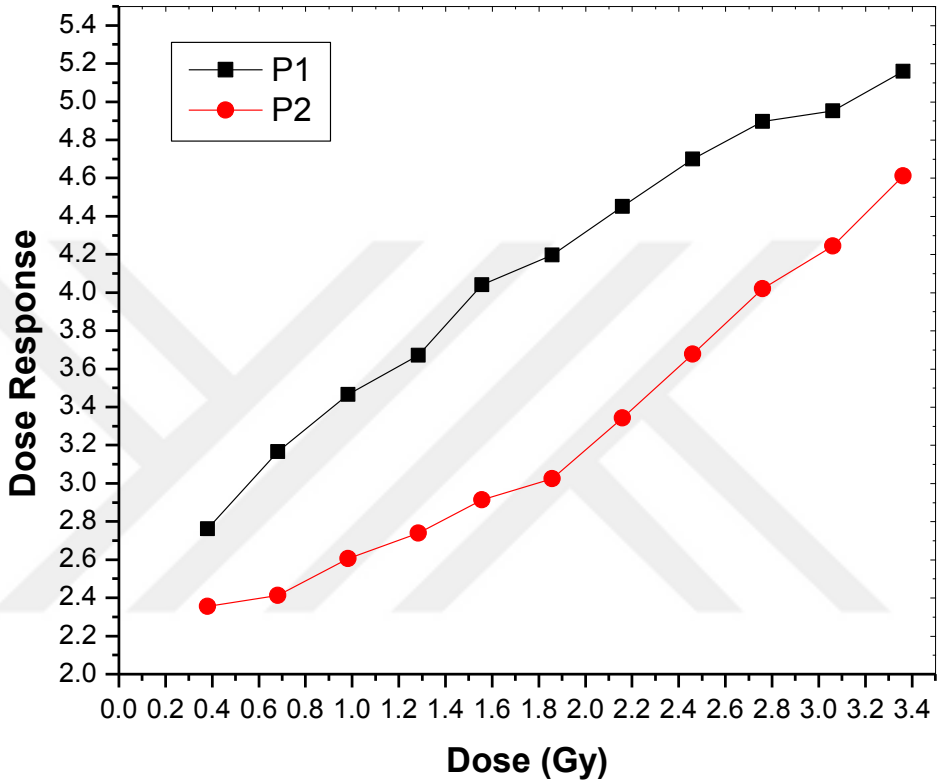


**Figure 6.8** The dose response of peak 1 and peak 2 determined by peak height method.

Complicating the glow curve analysis with the CGCD is very important method to detection the number of peaks included in the glow curve and finding the kinetic order of each glow peak to get the result. One of the most important features of the "CGCD" method is that it deals with complex glow curves. The least-squares function may receive incorrect kinetic attempts to determine the "best fit" for numerical data. Therefore, many possible combinations of kinetic parameters can be set to the same emission curve. In the current study, the first-order kinetic approximations are expressions for all “CGCD” evaluations, Eq.4.12. This method has become widespread method to determine kinetics parameters. F.O.M mean the figure of merit, this figure used for testing suitable fitting of the glow curve [58]. From many experiments the results indicate that if the F.O.M. values are between 0.0% to 2.5%

the fit is good , and if it from 2.5% to 3.5% it is fair fit, > 3.5% it is mean bad fit. In this study, when the evaluation of peaks 1 and 2 was followed by CGCD method, the third peak was observed at high temperature, when the calcite sample was irradiated by high doses up to 2 kGy. Calcite sample showed totally 3 peaks in this study, as seen in Fig.6.8.

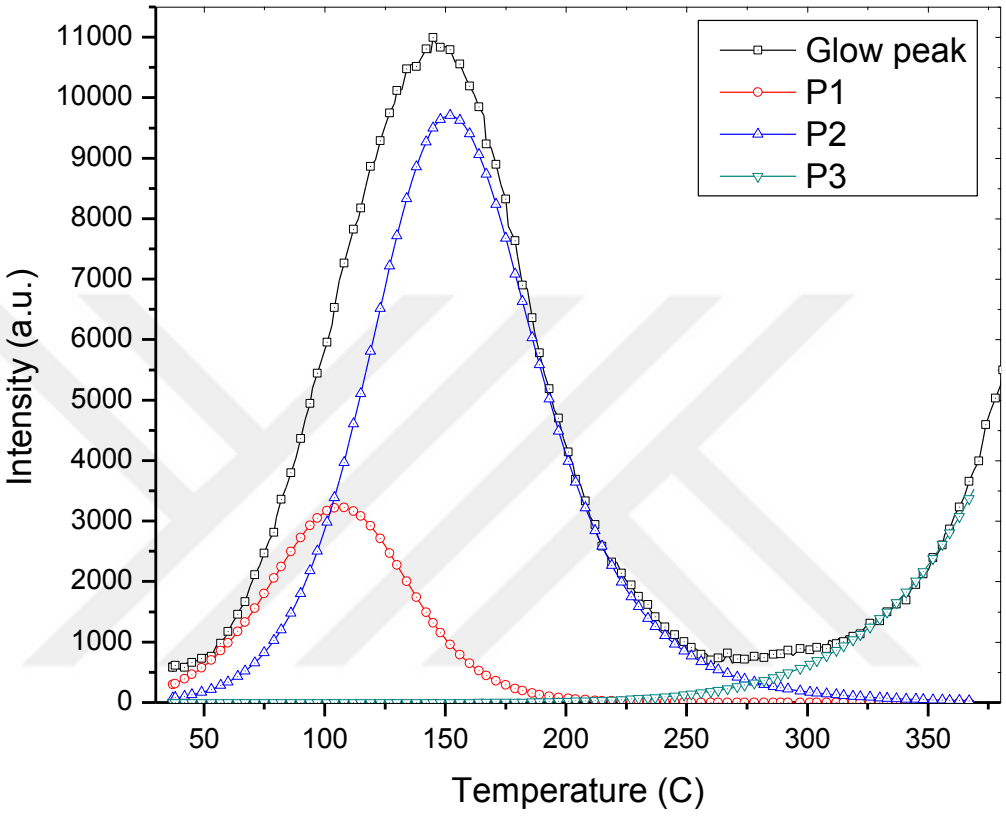


**Figure 6.9** The CGCD analyzes glow curve of calcite sample irradiated with dosage 36Gy.

# CHAPTER 7

# CONCLUSION

In this study, calcite sample was irradiated with Beta source between 2.4 Gy to 2.3 kGy at room temperature for investigate glow curves of calcite sample. Glow curve show two peaks at 189 °C and 280 °C for peak 1 and peak 2 respectively, third peak observed at high temperature. To estimate "b" value, peak shape (PS) method has been used and it found as general order kinetics. Activation energies were also calculated by using peak shape (PS), and (CGCD) computer glow curve deconvolution methods.

Gartia, Singh & Mazumdar peak shape method for three ratio of intensity (1/2I, 2/3I, 4/5I) gives values of E with little different to each other, it about 0.31 eV in the ratio, but Chen peak shape (PS) method estimate E value equal to 0.41 eV, that mean Chen peak shape method gives E value approximately 26% higher than Mazumder peak shape method, while CGCD method gives E value higher than Chen and Mazumdar peak shape (PS) method, it found about 0.5 eV component.

According to thermoluminescence theory by heating rate procedure, in the case of increasing heating rate the peak intensity must reduce and shifting to high temperature. But in this study show different result, this difference in results is due to the uncontrolled random distribution of the traps for natural calcite sample. Dose response for calcite sample components have same pattern, the linearity was followed in the first and then become saturated at different levels of dose.

After calcite sample irradiated by beta source for dose level about 36 Gy then stored in dark box at room temperature and read out after 1 hour, for the peak 1, the glow peak intensity turned to half of the original value, after stored for three week peak 1 disappeared from glow curve, when it stored for 1 day glow peak intensity found decreased to 12% of its original value.

## REFERENCES


[1] McKeever, S. W. S. (1985). Thermoluminescence of Solids, Cambridge, Univ. Press Cambridge, 32.

[2] Chen, R., & McKeever, S. W. (1997). Theory of thermoluminescence and related phenomena. World Scientific

[3] Chen, R., & Kirsh, Y. (2013). The analysis of thermally stimulated processes. Elsevier.

[4] McKeever, S. W. S., & Chen, R. (1997). Luminescence models. Radiation Measurements, **27**(5), 625-661.

[5] Furetta, C., & Weng, P. S. (1998). Operational thermoluminescence dosimetry. World Scientific Publishing Co Inc

[6] Bräunlich, P. (1979). Thermally stimulated relaxation in solids. Thermally stimulated relaxation in solids.

[7] Chen, R., & McKeever, S. W. (1997). Theory of thermoluminescence and related phenomena. World Scientific

[8] Chen, R., & Kirsh, Y. (2013). The analysis of thermally stimulated processes. Elsevier.

[9] McKeever, S. W. S. (1985). Thermoluminescence of Solids, Cambridge, Univ. Press Cambridge, 32.

[10] Oberhofer, M., & Scharmann, A. (1981). Applied thermoluminescence dosimetry. Adam Hilger Ltd..

[11] Glasstone, S., Laidler, K. J., & Eyring, H. (1941). The theory of rate processes; the kinetics of chemical reactions, viscosity, diffusion and electrochemical phenomena (541.39). McGraw-Hill Book Company,.

[12] Curie, D. (1946). Luminescence in Crystals (Methuen, London, 1963). *Google Scholar.*

[13] Chen, R., & Kirsh, Y. (2013). The analysis of thermally stimulated processes. Elsevier

[14] Kim, K. B., & Hong, D. G. (2014). Kinetic parameters, bleaching and radiation response of thermoluminescence glow peaks separated by deconvolution on Korean calcite. *Radiation Physics and Chemistry*, ***103***, 16-21.

[15] Abdel-Razek, Y. A. (2016). Thermoluminescence dosimetry using natural calcite. *Journal of Taibah University for Science*, ***10***(2), 286-295.

[16] Yildirim, R. G., Kafadar, V. E., Yazici, A. N., & Gün, E. (2012). The analysis of thermoluminescent glow peaks of natural calcite after beta irradiation. *Radiation protection dosimetry*, ***151***(3), 397-402.

[17] Engin, B., & Güven, O. (2000). The effect of heat treatment on the thermoluminescence of naturally-occurring calcites and their use as a gamma-ray dosimeter. *Radiation measurements*, ***32***(3), 253-272.

[18] Urbina, M., Millan, A., Beneitez, P., & Calderon, T. (1998). Dose rate effect in calcite. *Journal of luminescence*, ***79***(1), 21-28.

[19] De Lima, J. F., Valerio, M. E. G., & Okuno, E. (2001). Thermally assisted tunneling: An alternative model for the thermoluminescence process in calcite. *Physical Review B*, ***64***(1), 014105.

[20] Ninagawa, K., Kitahara, T., Toyoda, S., Hayashi, K., Nishido, H., Kinjo, M., & Kawana, T. (2001). Thermoluminescence dating of the Ryukyu Limestone. *Quaternary Science Reviews*, ***20***(5), 829-833.

[21] Kalita, J. M., & Wary, G. (2014). Thermoluminescence study of X-ray and UV irradiated natural calcite and analysis of its trap and recombination level. *Spectrochimica Acta Part A: Molecular and Biomolecular Spectroscopy*, *125*, 99-103.

[22] Macedo, Z. S., Valerio, M. E. G., & de Lima, J. F. (1999). Thermoluminescence mechanism of $Mn^{2+}$, $Mg^{2+}$ and $Sr^{2+}$ doped calcite. *Journal of Physics and Chemistry of Solids*, ***60***(12), 1973-1981.

[23] Furetta, C. (2003). Handbook of thermoluminescence.

[24] McKeever, S. W. S. (1984). Thermoluminescence in quartz and silica. *Radiation Protection Dosimetry*, ***8***(1-2), 81-98.

[25] Steven Dutch, University of Wisconsin, Natural and Applied Science (2005).

[26] Catherine E.H. and A.G.Sharpe, Inorganic Chemistry, (2001).

[27] Yazici, A. N. (1998). The effect of pre-irradiation heat treatment on the evaluated trapping parameters of LiF: Mg, Ti (TLD-100). *Radiation protection dosimetry*, ***80***(4), 379-384.

[28] Adirovitch, E. I. (1956). La formule de Becquerel et la loi élémentaire du déclin de la luminescence des phosphores cristallins. *Journal de Physique et le Radium*, ***17***(8-9), 705-707.

[29] Haering, R. R., & Adams, E. N. (1960). Theory and application of thermally stimulated currents in photoconductors. *Physical Review*, ***117***(2), 451.

[30] Halperin, A., & Braner, A. A. (1960). Evaluation of thermal activation energies from glow curves. *Physical Review*, ***117***(2), 408

[31] Bull, R. K., McKeever, S. W. S., Chen, R., Mathur, V. K., Rhodes, J. F., & Brown, M. D. (1986). Thermoluminescence kinetics for multipeak glow curves produced by the release of electrons and holes. *Journal of Physics D: Applied Physics*, ***19***(7), 1321.

[32] Sakurai, T. (1995). New method for numerical analysis of thermoluminescence glow curves. *Journal of Physics D: Applied Physics*, ***28***(10), 2139

[33] Randall, J. T., & Wilkins, M. H. F. (1945, November). Phosphorescence and electron traps. I. The study of trap distributions. In *Proceedings of the Royal Society of London A: Mathematical, Physical and Engineering Sciences* **184**(365-389). The Royal Society.

[34] Horowitz, Y. S. (1984). Thermoluminescence and Thermoluminescent Dosimetry, v. 2.

[35] G.Kitis, J.M. Gomez-Ros and J.W.N. (1989). Tuyn J.Phys.D: Appl.Phys. 31, 2636.

[36] Pagonis, V., Mian, S., & Kitis, G. (2001). Fit of first order thermoluminescence glow peaks using the Weibull distribution function. *Radiation protection dosimetry*, ***93***(1), 11-17.

[37] Kececioglu, D. (1991). Reliability engineering handbook **1**. Prentice-Hall, Inc.

[38] Garlick, G. F. J., & Gibson, A. F. (1948). The electron trap mechanism of luminescence in sulphide and silicate phosphors. *Proceedings of the physical society*, ***60***(6), 574.

[39] Bos, A. J. J., & Dielhof, J. B. (1991). The analysis of thermoluminescent glow peaks in CaF2: Tm (TLD-300). *Radiation protection dosimetry*, ***37***(4), 231-239.

[40] May, C. E., & Partridge, J. A. (1964). Thermoluminescent kinetics of alpha-irradiated alkali halides. *The Journal of Chemical Physics*, ***40***(5), 1401-1409.

[41] Chen, R., & Winer, S. A. A. (1970). Effects of various heating rates on glow curves. *Journal of applied physics*, ***41***(13), 5227-5232

[42] Chen, R. (1969). On the calculation of activation energies and frequency factors from glow curves. *Journal of Applied Physics*, *40*(2), 570-585.

[43] Burgkhardt, B., Singh, D., & Piesch, E. (1977). High-dose characteristics of CaF2 and CaSO4 thermoluminescent dosimeters. *Nuclear Instruments and Methods*, ***141***(2), 363-368.

[44] Grossweiner, L. I. (1953). A note on the analysis of first-order glow curves. *Journal of Applied Physics*, ***24***(10), 1306-1307.

[45] Halperin, A., & Braner, A. A. (1960). Evaluation of thermal activation energies from glow curves. *Physical Review*, ***117***(2), 408.

[46] Medlin, W. L. (1964). Trapping centers in thermoluminescent calcite. *Physical Review*, ***135***(6A), A1770.

[47] Lushchik C.B., Phys. 3, 408, (1960).

[48] Chen, R. (1969). Glow curves with general order kinetics. *Journal of the Electrochemical Society*, ***116***(9), 1254-1257.

[49] Balarin, M. (1979). Temperaturee Dependence of the Pre-Exponential Factor in the Glow Curve Theory. *physica status solidi (a)*, ***54***(2).

[50] Kathuria, S. P., & Sunta, C. M. (1979). Kinetics and trapping parameters of thermoluminescence in LiF TLD-100-dependence on dose. *Journal of Physics D: Applied Physics*, ***12***(9), 1573.

[51] Bos, A. J. J., Piters, J. M., Ros, J. G., & Delgado, A. (1993). IRI-CIEMAT Report 131-93-005. *IRI Delft*.

[52] Mahesh, K., Weng, P. S., & Furetta, C. (1989). Thermoluminescence in Solids and its Applications. Nuclear Technology Pub..

[53] Hsu, P. C., & Wang, T. K. (1986). On the annealing procedure for CaF2: Dy. *Radiation protection dosimetry*, ***16***(3), 253-256.

[54] 9010 Optical Dating System User Manual, Dec. 1993

[55] Model 3500 Manual TLD Reader User's Manual, July 30 1994, Publication No 3500-0-U-0793-005

[56] Kirsh, Y. (1992). Kinetic analysis of thermoluminescence. *physica status solidi (a)*, ***129***(1), 15-48.

[57] Singh, T. S. C., Mazumdar, P. S., & Gartia, R. K. (1988). On the determination of activation energy in thermoluminescence by the initial rise method. *Journal of Physics D: Applied Physics*, ***21***(8), 1312.

[58] Misra, S. K., & Eddy, N. W. (1979). IFOM, a formula for universal assessment of goodness-of-fit of gamma ray spectra. *Nuclear Instruments and Methods*, ***166***(3), 537-540.